AER/AGS Report 96

Numerical Groundwater Flow Model of the Sylvan Lake Sub-Basin in the Edmonton–Calgary Corridor, Central Alberta

AER/AGS Report 96

Numerical Groundwater Flow Model of the Sylvan Lake Sub-Basin in the Edmonton–Calgary Corridor, Central Alberta

J.E. Liggett and A. Singh

Alberta Energy Regulator
Alberta Geological Survey

November 2018

ISBN 978-1-4601-3973-8

Liggett, J.E. and Singh, A. (2018): Numerical groundwater flow model of the Sylvan Lake sub-basin in the Edmonton–Calgary Corridor, central Alberta; Alberta Energy Regulator / Alberta Geological Survey, AER/AGS Report 96, 41 p.

Published November 2018 by:
Alberta Energy Regulator
Alberta Geological Survey
4th Floor, Twin Atria Building
4999 – 98th Avenue
Edmonton, AB T6B 2X3
Canada

Tel: 780.638.4491
Fax: 780.422.1459
E-mail: AGS-Info@aer.ca
Website: www.ags.aer.ca/

Contents

Tables

Figures

Acknowledgements

The authors wish to thank L. Atkinson (Alberta Geological Survey [AGS]) for helpful discussion regarding the hydrostratigraphic model developed for the Sylvan Lake area and B. Smerdon (AGS) for valuable assistance, support, and discussion regarding the numerical modelling process. An early version of the Sylvan Lake numerical model was developed by P. Vermeulen (Deltares) and informed the conceptual model of the numerical model described in this report. Alberta Agriculture and Forestry (AAF) provided data from their Alberta Climate Information Service and from monitoring wells (used within AAF for specific applied research purposes). Finally, we would like to thank G.F. Huff (AGS) and B. Smerdon for helpful reviews of this report.

Abstract

The impact of increasing population and competing groundwater uses in the Sylvan Lake sub-basin is of concern to local stakeholders. A numerical groundwater flow model was developed in the United States Geological Survey's MODFLOW groundwater modelling software to improve the understanding of regional groundwater movement and availability, and to examine the effects of stresses on flow (e.g., pumping, change in groundwater recharge) and the broad-scale interaction of groundwater with surface water, including Sylvan and Gull lakes. The numerical model simulates flow within 10 hydrostratigraphic units, from the base of the Wapiti Formation to the surficial Neogene–Quaternary sediments. Previous geological modelling of sandstone abundance in the uppermost bedrock unit (i.e., Paskapoo Formation) was incorporated in the numerical model to account for the heterogeneity and connectedness of areas potentially having higher hydraulic conductivity. Both steady-state and transient flow conditions were considered. In the transient model, Sylvan and Gull lakes were represented using MODFLOW's lake package in order to assess lake–groundwater interactions. The model was calibrated based on lake level and observation well data, although transient observation well data were limited. Model input files are available for water management planning, scenario modelling, and increasing the knowledge of groundwater flow in the Sylvan Lake sub-basin.

1 Introduction

The numerical groundwater flow model described in this report was developed as part of the Provincial Groundwater Inventory Program (PGIP), a joint partnership between Alberta Environment and Parks (AEP) and the Alberta Geological Survey (AGS). The activities of PGIP include regional hydrogeological assessments and geological characterization projects, which aim to provide conceptualizations of surface and subsurface systems at basin and sub-basin scales. Developing these conceptualizations involves modelling the geological framework, describing how the geology translates into hydrostratigraphy (i.e., the relative ability of specific units to transmit and store water), and quantifying the movement of groundwater and its broad-scale interaction with surface water through groundwater flow modelling.

The Edmonton–Calgary Corridor (ECC) was the first region of interest for PGIP and a groundwater atlas (Barker et al., 2011) was produced to provide geological and hydrogeological information for regional planners, regulators, policy-makers, and the public. One of the priorities for stakeholders in the ECC is the increasing demand on water resources in the vicinity of Sylvan Lake. For example, the town of Sylvan Lake has an increasing population and is a popular tourist destination, which places pressure on natural resources due to development. Additionally, unconventional hydrocarbon resource development (Duvernay Formation in the East Shale Basin) has recently emerged in the area, which may increase demand on water resources. To characterize hydrogeological conditions at a finer resolution, the 5933 km^2 Medicine–Blindman subwatershed (Water Survey of Canada [WSC] watershed code 05CC) was prioritized for geological and hydrogeological modelling. This subwatershed is referred to as the Sylvan Lake sub-basin (SLSB) in this report (Figure 1).

1.1 Purpose and Scope

This report describes the construction, calibration, and results of a numerical model of groundwater flow in the SLSB. The purpose of this model is to improve the understanding of groundwater movement and availability. This model is a foundation for subsequent modelling of the SLSB, which could focus on specific water resource questions for either the entire sub-basin or more local areas of interest within the sub-basin. The model is available from the AGS for stakeholders to further develop as a decision support tool for water management planning and scenario modelling, and to increase knowledge of groundwater flow in the SLSB. The model simulates steady-state and transient flow conditions and is intended to support regional water resource planning and regulation. As a regional-scale model, groundwater movement, the effect of stress on flow (e.g., pumping, change in groundwater recharge), and broad-scale interaction of groundwater with surface water is represented.

Previous hydrostratigraphic modelling informs the construction of a conceptual and numerical model for groundwater in the SLSB. The current study combines data from two recent hydrostratigraphic projects (Lyster and Andriashek, 2012; Atkinson and Glombick, 2015a) as a means of representing heterogeneity of the shallowest bedrock formation (Paskapoo Formation) in the SLSB model. The description of the SLSB groundwater flow model includes information on the spatial and temporal discretization of the hydrogeological system, boundary conditions, stresses, and hydraulic properties. The sensitivity of the steady-state numerical simulation is documented and the transient model behaviour is described.

1.2 Study Area

The 5933 km^2 SLSB, located in central Alberta, lies primarily within NTS 83B, with much smaller portions lying in NTS 83A, 82O, and 82P (Figure 1). The Western Alberta Plains physiographic region comprises much of the SLSB and can be divided into a number of smaller districts such as the rolling hills of the Bucklake Upland in the northwest, and the gentle slopes and broad depressions of the Medicine River Plain in the central portion (Figure 2; Pettapiece, 1986). Considering the natural regions of Alberta (Natural Regions Committee, 2006), the SLSB lies within parts of the Lower Foothills, Central and Dry Mixedwood, and Central Parkland natural subregions (Figure 2).

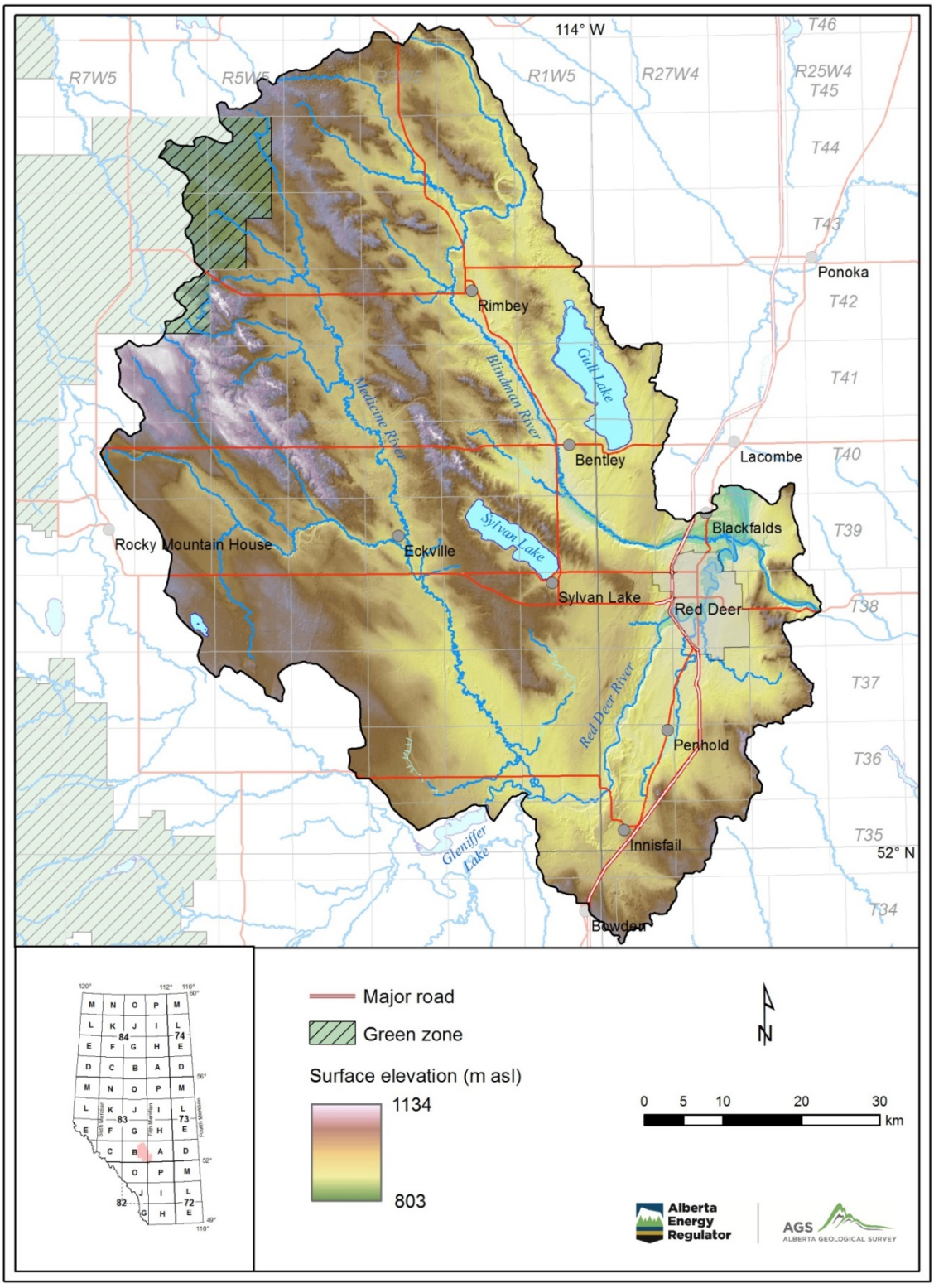

Figure 1. Sylvan Lake sub-basin (Water Survey of Canada watershed code 05CC) in the Edmonton–Calgary Corridor, central Alberta. The green zone is the forested portion of public land in Alberta.

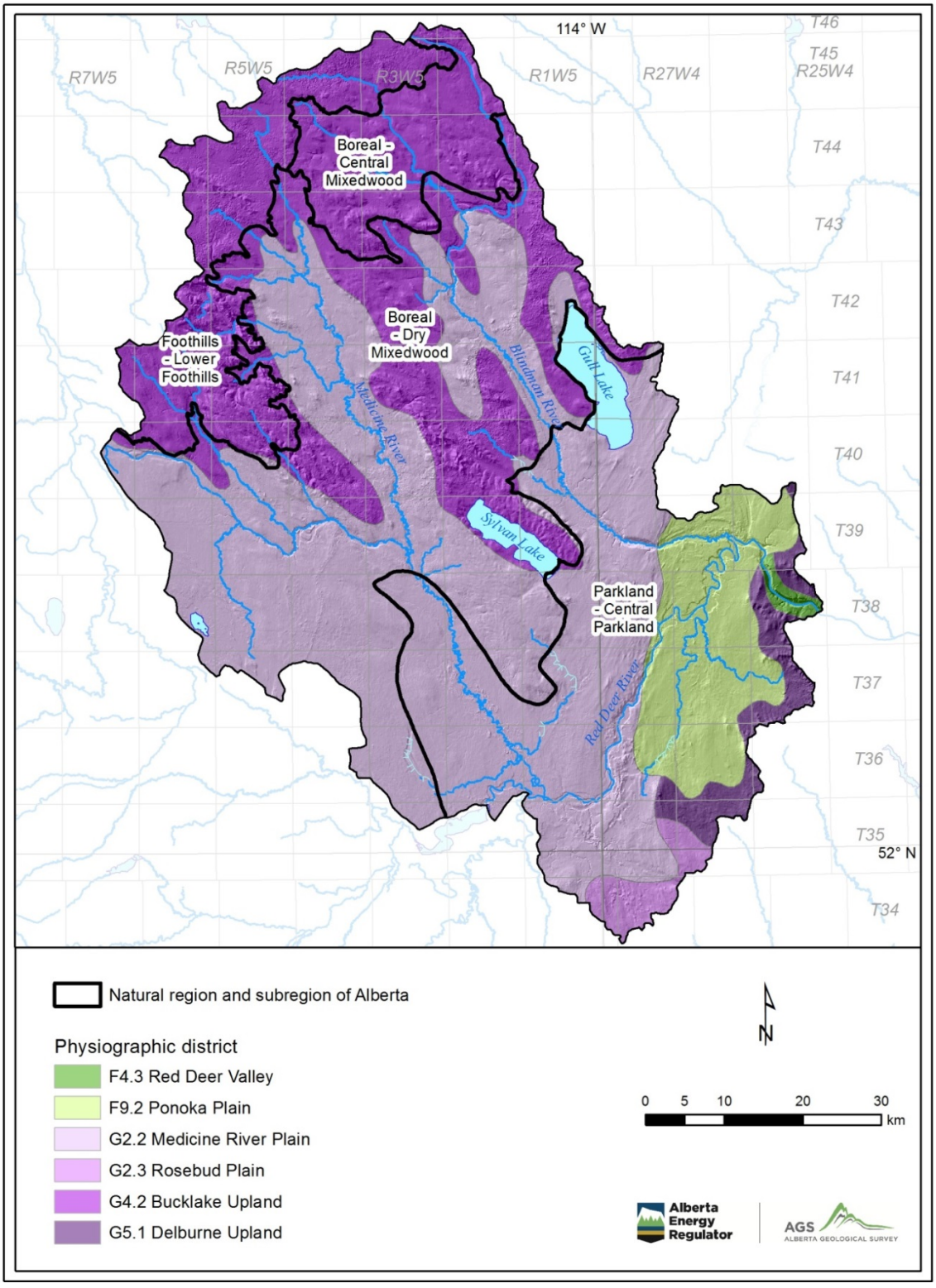

Figure 2. Physiographic districts and natural subregions of the Sylvan Lake sub-basin, central Alberta. Physiographic districts shown in purple and green are part of the Western and Eastern Alberta plains regions, respectively (Pettapiece, 1986). Map labels indicate the name of the natural region and subregion (Natural Regions Committee, 2006).

Much of the landscape in the study area is used for agriculture, with the exception of the forested headwaters of the Medicine and Blindman rivers in the northwestern margin, the urban areas along Highway 2 (e.g., Innisfail, Red Deer), and the town of Sylvan Lake.

The climate of the SLSB is continental, with warm summers and cold winters. The 1981–2010 normal mean annual air temperature at the Red Deer Airport is 2.8°C, with a mean daily maximum of 22.7°C in July and −5.5°C in January (Environment Canada, 2015). Normal mean annual precipitation is 497 mm/yr for 1981–2010, with an annual mean of 120 mm/yr of precipitation falling as snow.

The Medicine–Blindman subwatershed, which defines the SLSB study area, is within the upper portion of the Red Deer River basin and contains the Medicine, Blindman, and Red Deer rivers (Figure 3). The Medicine River joins the Red Deer River just downstream of Gleniffer Lake, and has a mean annual flow of 4.6 m^3/s at Eckville (WSC hydrometric station number 05CC007), calculated from the historical flow data in WSC's Hydroclimatological Data Retrieval Program database (HYDAT; Water Survey of Canada, 2017). The meandering Blindman River has a mean annual flow of 3.0 m^3/s (station number 05CC001) where it joins the Red Deer River at Red Deer. The Red Deer River flows northeast and is dammed by the Dickson dam (creating Gleniffer Lake [reservoir]) just west of where the river enters the SLSB. Mean annual flow of the Red Deer River is 48.7 m^3/s (station number 05CC002). Figure 3 shows the drainage areas associated with each hydrometric station within the SLSB, as delimited by Agriculture and Agri-Food Canada's Watersheds Project (Agriculture and Agri-Food Canada, 2012). Only three hydrometric stations operate continuously throughout the year (stations 05CC001, 05CC002, 05CC007; Figure 3).

The SLSB contains Sylvan Lake and Gull Lake, both of which are popular for recreation. Gull Lake (~80 km^2) has a relatively small drainage area (~200 km^2) and drains through a creek into the Blindman River. Sylvan Lake (~43 km^2) also has a relatively small drainage area (~100 km^2) but surface water outflow only occurs intermittently, once the lake level reaches a minimum of 936.7 m above sea level (asl; Baker, 2009). As such, Sylvan Lake can be considered a closed-basin lake. The low ratio of drainage area to lake area for both Gull and Sylvan lakes (~2.6 and 2.4, respectively) suggests a strong connection with groundwater.

2 Hydrogeological Framework

The regional geology, hydrology, and hydrogeology of the SLSB has been described in previous PGIP mapping projects (Riddell et al., 2009; Barker et al., 2011; Riddell et al., 2014; Riddell and Lyster, 2017; Smerdon et al., 2017), AGS reports (Lyster and Andriashek, 2012; Atkinson and Glombick, 2015a), and research at the University of Calgary (Baker, 2009). The area has also been the focus of numerous regional consulting projects (e.g., Hydrogeological Consultants Ltd., 2001, 2005; AXYS Environmental Consulting Ltd., 2005), especially with regards to the water quality of Sylvan Lake. These projects have found that nonsaline groundwater in the SLSB is sourced from coarse-grained Neogene–Quaternary (N–Q) sediments, often located at the base of buried valley systems, and from shallow Upper Cretaceous−Paleogene bedrock formations.

Atkinson and Glombick (2015a) created a multilayer hydrostratigraphic model of the SLSB for the purpose of constructing a numerical model of groundwater flow. A total of 10 hydrostratigraphic units (HSU) were defined that describe both the N–Q sedimentary succession and Upper Cretaceous−Paleogene bedrock units (Figure 4). For each HSU, an elevation grid of the structure top was created with a 400 m cell size. The AGS drillcores (Riddell et al., 2009) and Alberta Water Well Information Database (AWWID; Alberta Environment and Parks, 2015a) were the primary data sources for N–Q sediments modelling, and digital gamma-ray well logs provided by the oil and gas industry were the primary data source for Upper Cretaceous−Paleogene bedrock modelling. A summary of the HSUs from Atkinson and Glombick (2015a) follows.

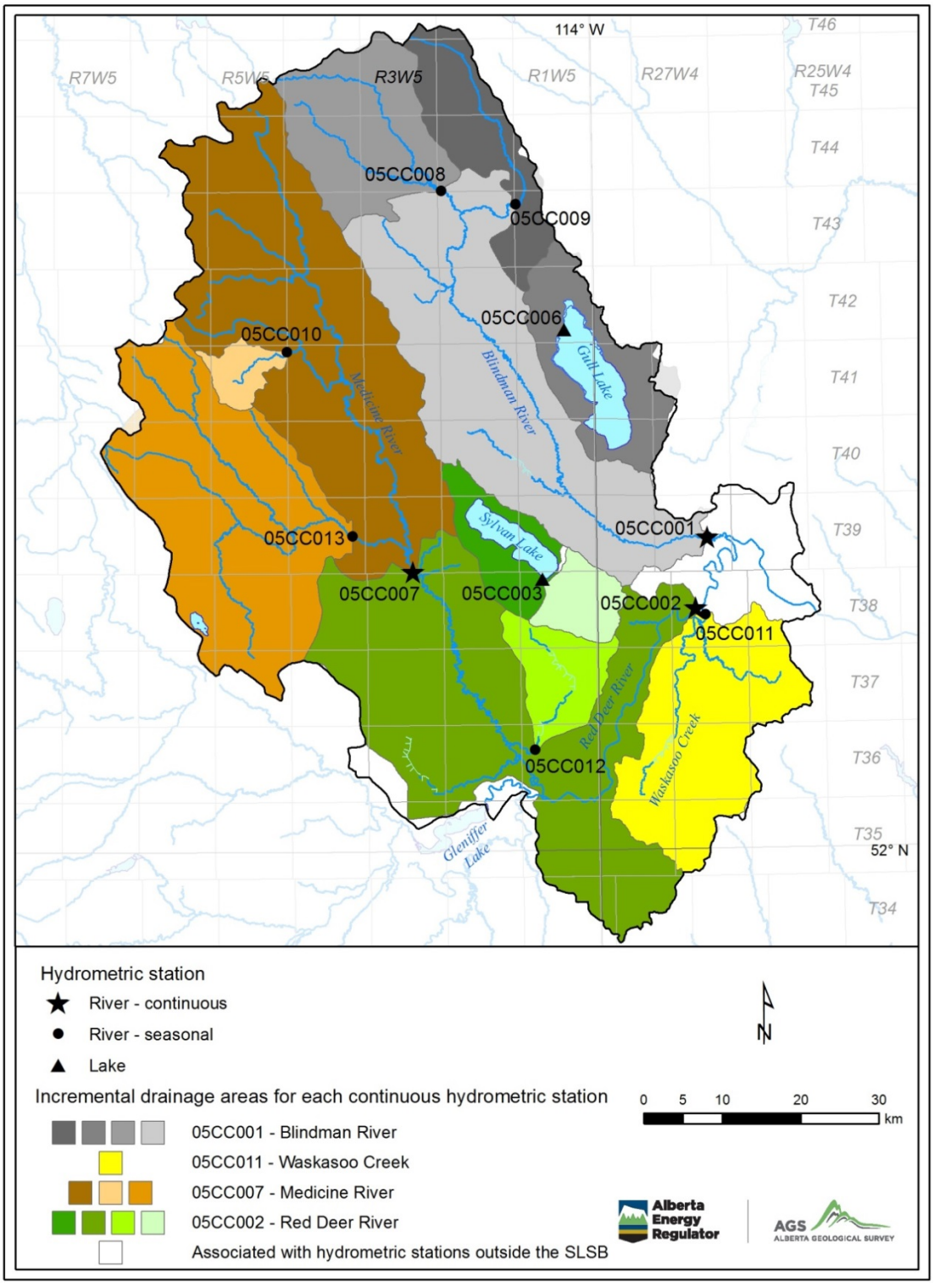

Figure 3. Incremental drainage areas associated with each Hydroclimatological Data Retrieval Program (HYDAT) hydrometric station, in the vicinity of the Sylvan Lake sub-basin (SLSB), central Alberta. Drainage areas in both orange and green are associated with hydrometric station 05CC002 along the Red Deer River. There are some differences between the boundaries of the incremental drainage areas and the boundary of the SLSB due to different data sources for watershed boundaries.

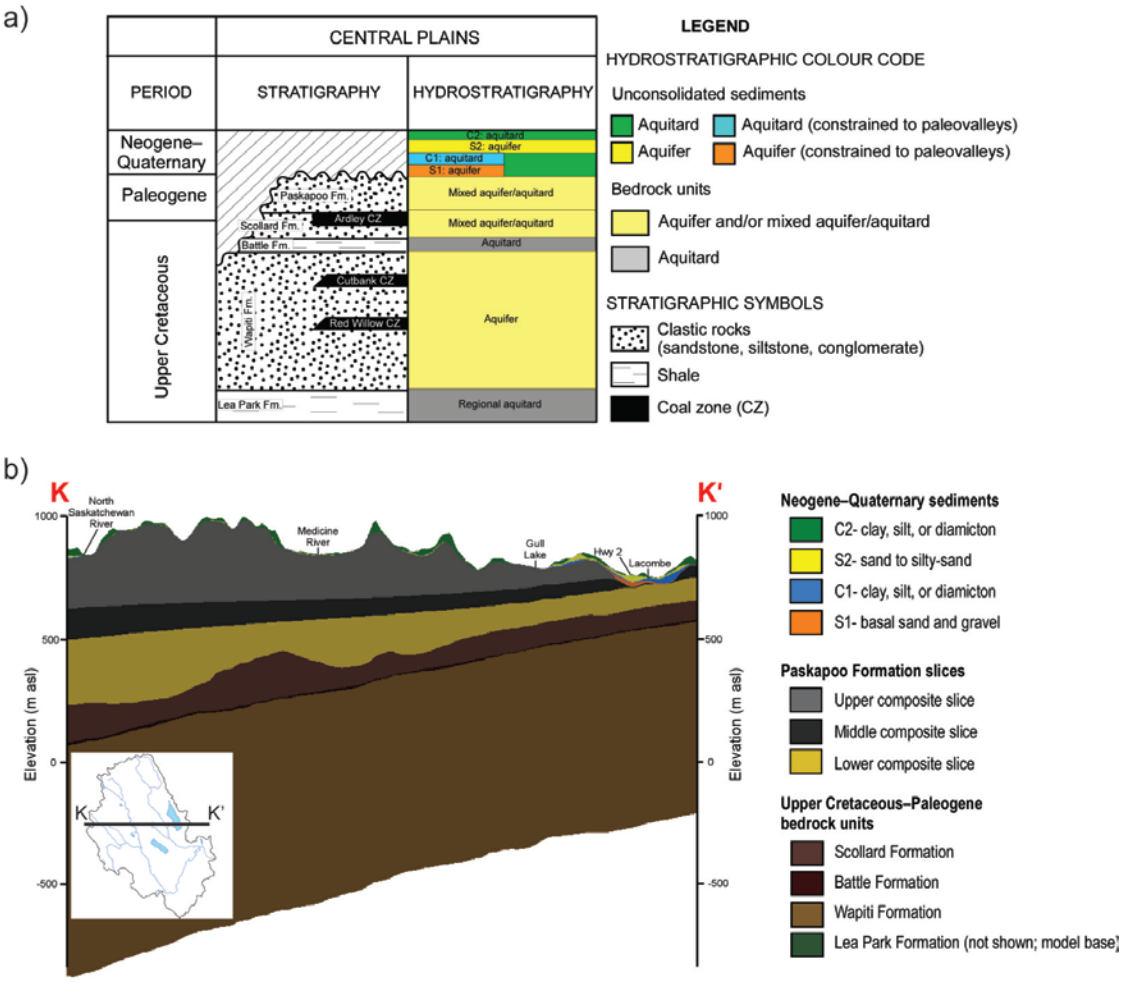

Figure 4. Hydrostratigraphy of the Sylvan Lake sub-basin (SLSB), central Alberta, from Atkinson and Glombick (2015a): a) hydrostratigraphic column and b) cross-section through the SLSB showing dipping bedrock and overlying Neogene–Quaternary sediments. The Paskapoo Formation was divided into three hydrostratigraphic units based on sandstone abundance.

In the bedrock succession, HSUs were defined on the basis of lithostratigraphic formation boundaries, with the exception of the subdivision of the Paskapoo Formation into three HSUs based on modelled sandstone abundance. The hydrostratigraphic model considers only those bedrock units above the Lea Park Formation, as this widespread fine-grained unit acts as a regional confining layer (Michael and Bachu, 2001) and is used as the base of the numerical groundwater model. Overlying the Lea Park Formation are the Wapiti, Battle, Scollard, and Paskapoo formations, which all dip in a westerly direction and thin eastwards (Figure 4). The Wapiti HSU (equivalent to the Wapiti Formation) consists of interbedded sandstone and siltstone, with minor mudstone and coal, deposited in a mainly fluvial environment with local areas of lacustrine influence (Dawson et al., 1994). The Wapiti HSU is generally considered an aquifer. The thin (up to 10 m), mudstone-dominated Battle HSU (equivalent to the Battle Formation) acts as an aquitard, confining the Wapiti HSU throughout much of the study area; however, the Battle HSU is absent in parts of the southeastern SLSB, having been eroded in paleovalleys trending southeast (Hathway, 2011; Atkinson and Glombick, 2015a). The overlying Scollard HSU (equivalent to the Scollard Formation) is an eastward-thinning wedge of nonmarine fluvial sedimentary rocks. It generally consists of thick grey to buff sandstone and siltstone units, interbedded with thin, olive-green mudstone beds and coal (Dawson et al., 1994); hence, the Scollard HSU is considered a mixed aquifer and aquitard (Atkinson and Glombick, 2015a). Finally, the Paskapoo Formation is a Paleogene fluvial

deposit characterized by stacked, multistorey, channel sandstone bodies that may coalesce to form semicontinuous sandstone sheets (Atkinson and Glombick, 2015a). These sandstone units are surrounded by either siltstone or mudstone. The Paskapoo Formation covers over 65 000 km^2 of southwestern Alberta and is the uppermost bedrock unit over its area of occurrence (Chen et al., 2007). This formation is the most important nonsaline groundwater source in the Canadian Prairies.

Hydrogeological characteristics of the Paskapoo Formation have been described by Grasby et al. (2008), Lyster and Andriashek (2012), and Atkinson and Glombick (2015a). Lyster and Andriashek (2012) used the AWWID and digital gamma-ray well logs provided by the oil and gas industry to model sandstone abundance (i.e., net-to-gross ratio [NGR]) within the Paskapoo Formation and generate a detailed representation of the architecture of sandstone bodies within the formation. They suggested three informal HSUs, roughly equivalent to the three formal lithostratigraphic members defined by Demchuk and Hills (1991): the Haynes aquifer (Haynes Member), the Lacombe aquitard (Lacombe Member), and the Sunchild aquifer (Dalehurst Member). Atkinson and Glombick (2015a) modified the approach used by Lyster and Andriashek (2012) and also divided the Paskapoo Formation in the SLSB into three HSUs based on the relative abundance of sandstone within a series of subsurface slices. The three HSUs of the Paskapoo Formation include a lower unit with generally high NGRs (majority between 0.50 and 0.90), and middle and upper units with lower NGRs (majority between 0.20 and 0.60; Figure 5; Atkinson and Glombick, 2015a). These slices likely correlate with the Haynes aquifer, Lacombe aquitard, and Sunchild aquifer, which were previously identified by Lyster and Andriashek (2012); although Atkinson and Glombick (2015a) interpreted less sandiness in the upper unit (i.e., the Sunchild aquifer) due to differences in the geological data used and interpretation method.

The N–Q sediments in the study area are heterogeneous and vary in thickness from 0 to 130 m, with greater thicknesses in the vicinity of the city of Red Deer (Atkinson and Glombick, 2015a). Atkinson and Glombick (2015a) delineated four HSUs in the N–Q sediments on the basis of texture and relative position in the subsurface (Figure 6). The four HSUs consist of S1, a coarse-grained (sand and gravel) basal unit, directly overlying bedrock and constrained to paleovalleys; C1, a fine-grained diamicton underlying S2; S2, coarse-grained discontinuous sand bodies; and C2, a fine-grained diamicton (Figure 6; Atkinson and Glombick, 2015a). The C1 and C2 HSUs may be indistinguishable where S2 HSU is absent. The N–Q sediments are important domestic sources of water and S1 HSU is referred to informally as the Red Deer basal aquifer. North of the city of Red Deer, sand and gravel deposits closer to the ground surface are mined as aggregate.

Across the ECC, groundwater recharge decreases eastwards and southeastwards in response to decreasing precipitation (Riddell et al., 2014). Within the SLSB, mean annual precipitation (January 1963 to March 2014) is 531 mm in the west (weather station Leedale AGDM), and 442 mm in the east (weather station Lacombe CDA 2; Alberta Agriculture and Forestry, 2014).

Previous mapping of vertical gradients and regional recharge and discharge areas (Barker et al., 2011; Riddell and Lyster, 2017) also helped inform the development of the numerical model of groundwater flow. Groundwater flow in the SLSB occurs at local and regional scales. At the local scale, groundwater is recharged in upland areas and discharges in adjacent lowland areas, such as the Medicine and Blindman river valleys, and Sylvan and Gull lakes. These local groundwater flow systems develop in both the unconsolidated deposits of the N–Q sedimentary succession, and shallow portions of the Paskapoo Formation. Local-scale groundwater flow systems are superimposed on regional-scale groundwater flow, which circulates through the deeper bedrock. At the regional-scale, groundwater is recharged in the foothills of the Rocky Mountains to the west and flows east through the Paskapoo, Scollard, and Wapiti HSUs before discharging to larger rivers such as the Red Deer, North Saskatchewan, and Bow. This conceptual model of regional flow was demonstrated in a regional-scale groundwater flow model developed by the AGS, which extends across southern Alberta and southwestern Saskatchewan (Singh et al., 2014), and is apparent in provincial-scale mapping of hydraulic heads in the Wapiti HSU (Singh and Nakevska, in press).

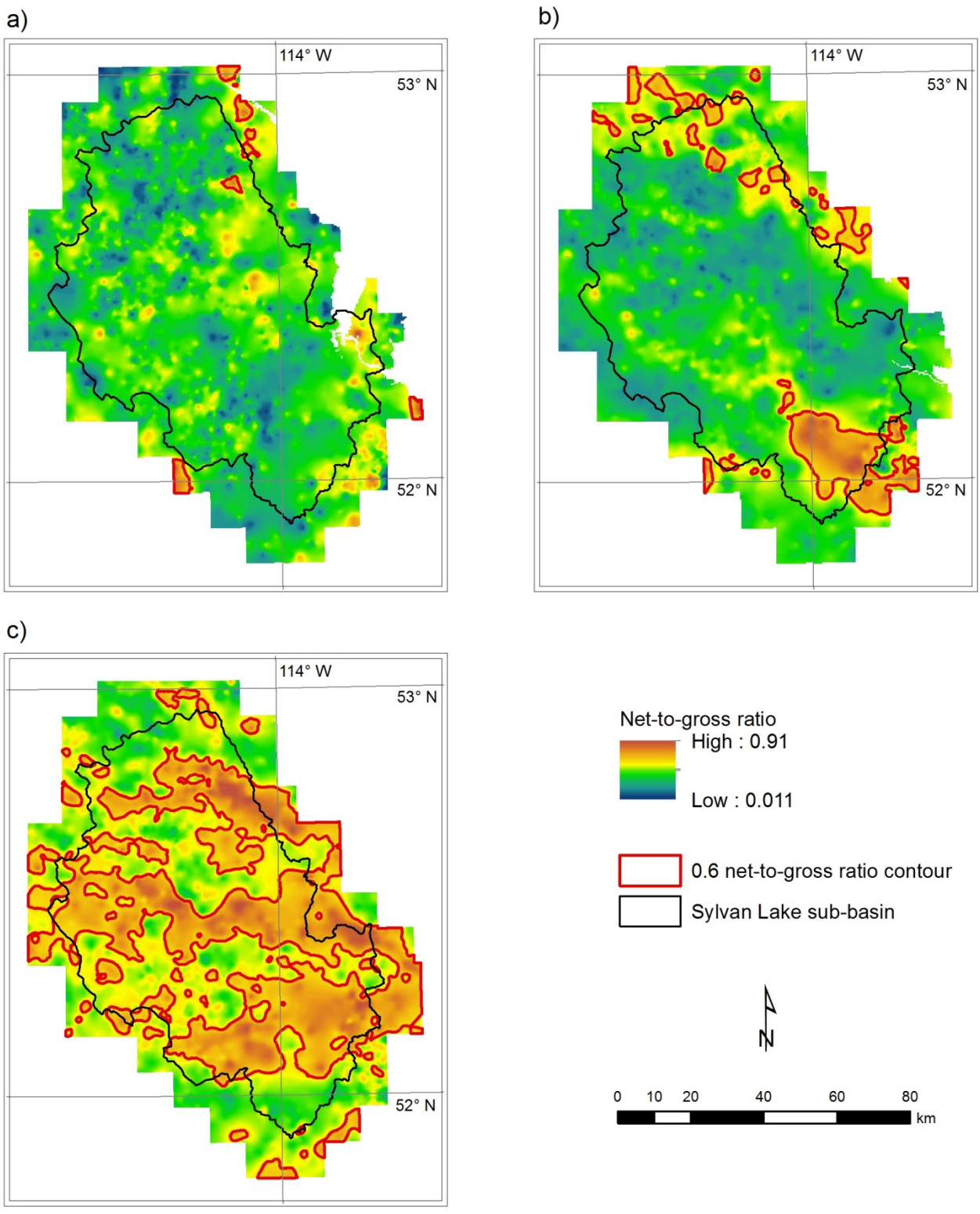

Figure 5. Plan view maps of net-to-gross sandstone ratio in each of the three Paskapoo Formation hydrostratigraphic units mapped by Atkinson and Glombick (2015a): a) upper Paskapoo, b) middle Paskapoo, and c) lower Paskapoo (Sylvan Lake sub-basin, central Alberta).

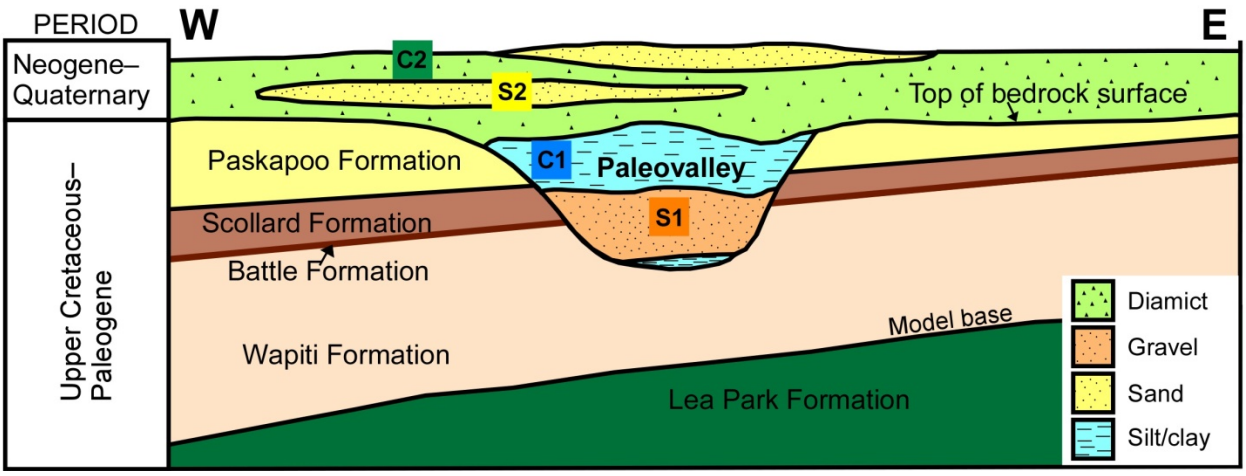

Figure 6. Conceptual model of the vertical succession of Neogene–Quaternary sediments overlying bedrock in the Sylvan Lake sub-basin, central Alberta. Units are not to scale. From Atkinson and Glombick (2015a).

A prominent hydrological feature in the SLSB is Sylvan Lake. The lake's connection to groundwater was studied by Baker (2009). Using three separate mass balances (chloride, deuterium, and oxygen-18), Baker (2009) found that rates of groundwater inflow and outflow were 27 to 35% of the total annual lake water budget, which corresponded to an average lake water residence time of 20 to 35 years. The average rate of groundwater inflow and outflow was 13.3×10^6 m^3/yr and 15.4×10^6 m^3/yr, respectively. Baker (2009) suggested that interaction between Sylvan Lake and groundwater was constrained to locations where a high abundance of sandstone within the Paskapoo Formation was close to the lakebed.

3 Numerical Model Setup

The numerical simulations for this study were made using the United States Geological Survey's (USGS) finite difference groundwater modelling software, MODFLOW-NWT (Niswonger et al., 2011). The pre- and post-processing for the study was done using Visual MODFLOW Classic (Waterloo Hydrogeologic, 2016), iMOD (Deltares, 2015), and ArcGIS (Esri, 2012). Both a steady-state and transient version of the model was developed, and the calibration of the steady-state model informed the input parameters used in the transient model.

3.1 Model Domain and Layering

The entire numerical model domain is 127.6 km in the x-direction (east–west) and 142.5 km in the y-direction (north–south) with the bottom-left corner at 489900 E and 5727000 N (NAD83, 10TM AEP Forest projection; Figure 7). The boundary between the inactive and actively modelled portions of the domain (i.e., the 'model boundary') varies with depth in order to assign appropriate flow boundaries to the model edges (Figure 7). In the N–Q sediments and upper Paskapoo HSUs, the model boundary was defined based on the surface area of the Medicine–Blindman subwatershed, reflecting the influence of surface topography in creating local groundwater flow systems and groundwater divides. For the middle Paskapoo HSU and deeper, the model boundary was defined based on lines of equipotential taken from the regional model of Alberta by Singh et al. (2014), in order to reflect the regional flow systems in deeper units. The two portions of the model are referred to in the remainder of this report as the 'shallow domain' and 'deep domain', respectively. The spatial extent of the deep domain is larger than the shallow domain and provides a buffer between the shallow domain extent and the boundary applied to the deep domain based on the regional model by Singh et al. (2014). The dominant area of interest in the SLSB model is that which lies within the lateral extent of the shallow domain.

a)

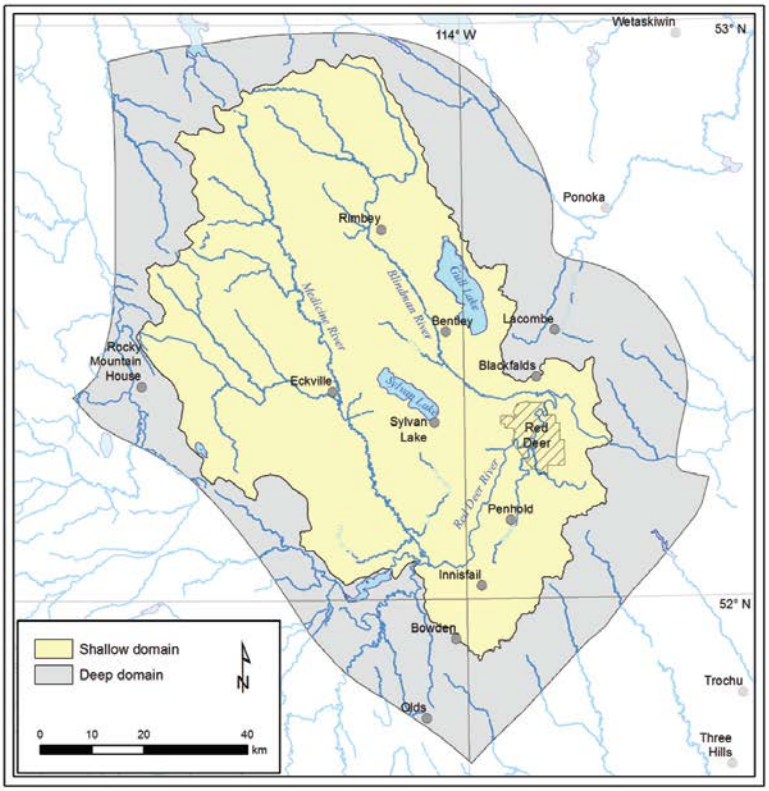

b)

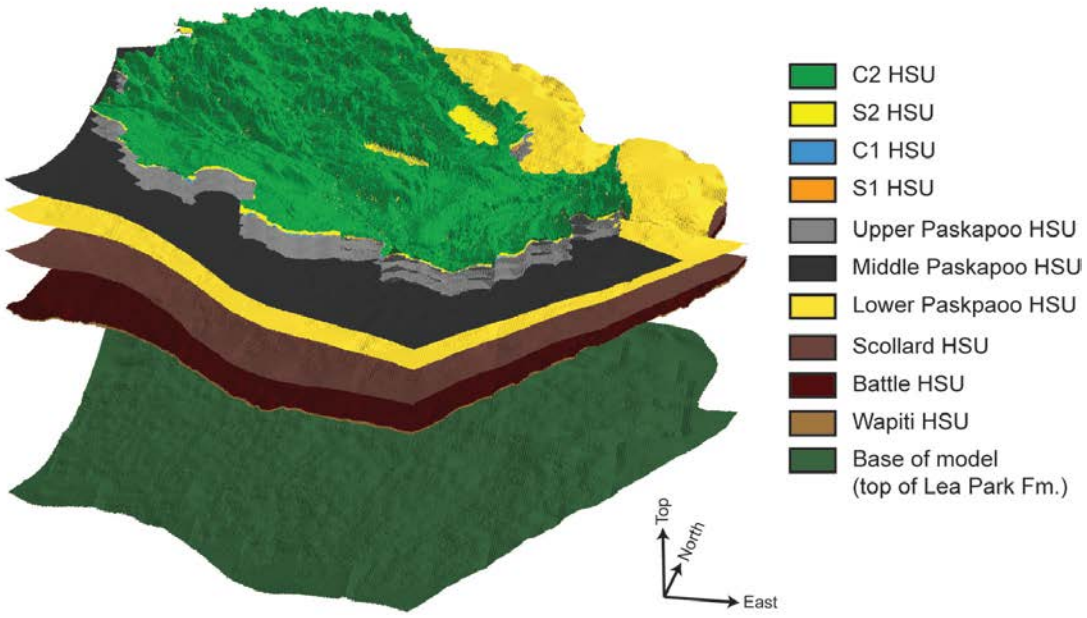

Figure 7. Active domain of the numerical model of the Sylvan Lake sub-basin, central Alberta. a) Plan view of the extent of the shallow and deep model domains. The shallow domain is coincident with the surface area of the Medicine–Blindman subwatershed and the deep domain follows lines of equipotential from the regional model of Alberta by Singh et al. (2014). b) Three-dimensional view of the model domain. Surfaces shown represent the top of each HSU. Vertical exaggeration is 50 times.

The numerical model was discretized laterally into cells of 200 by 200 m that align with the 400 by 400 m hydrostratigraphic model surfaces and allow definition of finer-scale flow fields relevant in the near surface. Vertically, the numerical model was discretized into 13 layers (Table 1, Figure 7b), mostly following the hydrostratigraphic model developed by Atkinson and Glombick (2015a). However, in addition to the three main HSUs of the Paskapoo Formation (upper, middle, and lower), the upper Paskapoo HSU is split into four model layers (layers 5–8, Table 1). This allows the extent of the Sunchild aquifer mapped by Lyster and Andriashek (2012), which was not as well defined by Atkinson and Glombick (2015a) due to different geological modelling methods, to be considered in the numerical model. The addition of multiple model layers within the upper Paskapoo HSU also allows for refinement of the near-surface hydraulic gradients, which is required to adequately represent shallow groundwater circulation and for future consideration of additional hydrological processes (e.g., evapotranspiration, interaction with surface water).

Table 1. Numerical model layers, Sylvan Lake sub-basin, central Alberta. Each layer is generally attributed to a particular hydrostratigraphic unit (HSU) and a minimum grid thickness of 0.1 m was used if that HSU was absent in a given area. Abbreviation: N–Q, Neogene to Quaternary.

Model Layer Number	Layer Name		Elevation Data Source for Top of Layer
1	C2 HSU	N–Q sediments	Atkinson (2015a)
2	S2 HSU		Atkinson (2015b)
3	C1 HSU		Atkinson (2015c)
4	S1 HSU		Atkinson (2015d)
5	Upper Paskapoo 1	Upper Paskapoo HSU	Atkinson (2015e)
6	Upper Paskapoo 2		5 m from top of upper Paskapoo HSU from Atkinson (2015e)
7	Upper Paskapoo 3		50 m from top of upper Paskapoo HSU from Atkinson (2015e)
8	Upper Paskapoo 4		100 m from top of upper Paskapoo HSU from Atkinson (2015e)
9	Middle Paskapoo HSU		Atkinson and Glombick (2015b), extended based on data trend
10	Lower Paskapoo HSU		Atkinson and Glombick (2015c), extended based on data trend
11	Scollard HSU		Atkinson and MacCormack (2015a), extended based on data trend
12	Battle HSU		Atkinson and MacCormack (2015b), extended based on 2015 AGS provincial bedrock framework mapping (K. MacCormack, pers. comm., 2015)
13	Wapiti HSU		Atkinson and MacCormack (2015c), extended based on 2015 AGS provincial bedrock framework mapping (K. MacCormack, pers. comm., 2015)
Base	Top of Lea Park Formation		Atkinson and MacCormack (2015d), extended based on 2015 AGS provincial bedrock framework mapping (K. MacCormack, pers. comm., 2015)

The elevations of the tops of the layers were taken directly from the published hydrostratigraphic model elevation surfaces (Table 1) described by Atkinson and Glombick (2015a) with the following exceptions. The upper Paskapoo HSU was divided into four model layers based on the distance from the top of the upper Paskapoo HSU defined by Atkinson and Glombick (2015a). The topmost layer of the upper Paskapoo HSU (i.e., model layer 5; Table 1) is 5 m thick, followed by a 45 m thick layer (i.e., model layer 6, from 5.1 to 50 m below the top of the upper Paskapoo HSU), a 50 m thick layer (i.e., model layer 7, from 50.1 to 100 m below the top of the upper Paskapoo HSU), and finally a layer of variable thickness reflecting depths greater than 100 m below the top of the upper Paskapoo HSU (i.e., model layer 8). The hydrostratigraphic model by Atkinson and Glombick (2015a) does not cover the entire lateral extent of the deep model domain, therefore the layer top elevations for the middle Paskapoo HSU and deeper were extended to cover the entire deep domain area based on either a subjective extension of the general trend of the surfaces (top of middle and lower Paskapoo HSUs, Scollard HSU), or by merging the surface described by Atkinson and Glombick (2015a) with mapped structure top surfaces from a November 2015 version (K. MacCormack, pers. comm., 2015) of the AGS's 3D provincial geological framework model (Battle, Wapiti, Lea Park formations). A minimum model layer thickness of 0.1 m was used where a particular HSU is absent.

3.2 Hydraulic Properties

Hydraulic properties are assigned for each model layer using a variety of data sources (Table 2). For the N–Q sediments HSUs and HSUs below the lower Paskapoo, hydraulic properties were assumed constant throughout the entire spatial extent of an HSU (Table 2). In the upper Paskapoo HSU, grid cells within the four model layers (layers 5–8) were compared to the location and thickness of the Sunchild aquifer mapped by Lyster and Andriashek (2012) (Andriashek and Lyster, 2012a,b). If the thickness of the Sunchild aquifer was greater than 60% of the thickness of the particular model grid cell, than that cell was considered as representative of the Sunchild aquifer, and assigned a higher hydraulic conductivity than the surrounding upper Paskapoo HSU grid cells. For the middle and lower Paskapoo HSUs, the distribution of hydraulic properties was based on the sandstone NGRs determined by Atkinson and Glombick (2015a,d–f). Areas with a NGR greater than 60% were considered as having a higher hydraulic conductivity than the rest of the HSU. Areas with only a few isolated grid cells of higher hydraulic conductivity were removed and areas with highly spatially varying hydraulic conductivity were simplified in order to reduce the computational burden on the numerical model. Values of horizontal (K_x, K_y) and vertical hydraulic conductivities (K_z) were based on previous studies, 59 historical pumping test results from original hard-copy water well drilling records (internal AGS data), and calibration of the models (Table 2; Section 4).

Figure 8 shows the hydraulic property zones for model layers 1, 2, and 5. As each model layer is representative of a particular HSU (Table 1); areas where that HSU is absent are assigned hydraulic properties of the HSU below. This corresponds to grid cells with a thickness of ≤0.1 m (i.e., the minimum thickness). The effect of this can be seen in Figure 8, where hydraulic properties from lower HSUs have been assigned to cells in the upper model layers. Figure 8c shows model layer 5, which is the topmost layer in the upper Paskapoo HSU. Hydraulic conductivity varies spatially in this layer based on the distribution of the Sunchild aquifer (hydraulic property zone 6).

For the transient model, the values for specific storage and specific yield are 0.0001 and 0.4, respectively. These values were selected during the manual calibration stage of the modelling process.

Table 2. Hydraulic properties used for each hydrostratigraphic unit (HSU) in the Sylvan Lake sub-basin numerical model. Abbreviation: K, hydraulic conductivity; K_x, K_y, horizontal hydraulic conductivity; K_z, vertical hydraulic conductivity; N–Q, Neogene to Quaternary.

Property Zone	Zone Name		Hydraulic Conductivity (Calibrated Value) K_x, K_y (m/s)	K_z (m/s)	Data Sources
1	Inactive cells				
2	C2 HSU	N–Q sediments	2.4×10^{-7}	6.0×10^{-10}	Regional model (Singh et al., 2014)
3	S2 HSU		1.0×10^{-4}	2.0×10^{-5}	Estimated to be higher than C1, C2
4	C1 HSU		2.4×10^{-6}	6×10^{-7}	Regional model (Singh et al., 2014)
5	S1 HSU		1.0×10^{-4}	2.5×10^{-5}	Estimated to be higher than C1, C2
6	Upper Paskapoo 1 – high K	Upper Paskapoo HSU	1.0×10^{-4}	2.6×10^{-5}	Grasby et al. (2008), Lyster and Andriashek (2012), Smerdon et al. (2017), historical pumping test results (internal AGS data)
7	Upper Paskapoo 1 – low K		8.0×10^{-5}	8.0×10^{-6}	
8	Upper Paskapoo 2 – high K		1.0×10^{-4}	2.6×10^{-7}	
9	Upper Paskapoo 2 – low K		1.0×10^{-6}	2.6×10^{-9}	
10	Upper Paskapoo 3 – high K		1.0×10^{-3}	2.6×10^{-6}	
11	Upper Paskapoo 3 – low K		1.0×10^{-6}	2.6×10^{-9}	
12	Upper Paskapoo 4 – high K		1.0×10^{-3}	2.6×10^{-6}	
13	Upper Paskapoo 4 – low K		1.0×10^{-6}	2.6×10^{-9}	
14	Middle Paskapoo HSU – high K	Middle Paskapoo HSU	1.0×10^{-3}	2.6×10^{-6}	
15	Middle Paskapoo HSU – low K		1.0×10^{-6}	2.6×10^{-9}	
16	Lower Paskapoo HSU – high K	Lower Paskapoo HSU	1.0×10^{-3}	2.6×10^{-6}	
17	Lower Paskapoo HSU – low K		1.0×10^{-4}	2.6×10^{-7}	
18	Scollard HSU		1.0×10^{-8}	1.0×10^{-9}	Regional model (Singh et al., 2014)
19	Battle HSU		1.0×10^{-10}	1.0×10^{-10}	
20	Wapiti HSU		9.0×10^{-9}	9.0×10^{-11}	

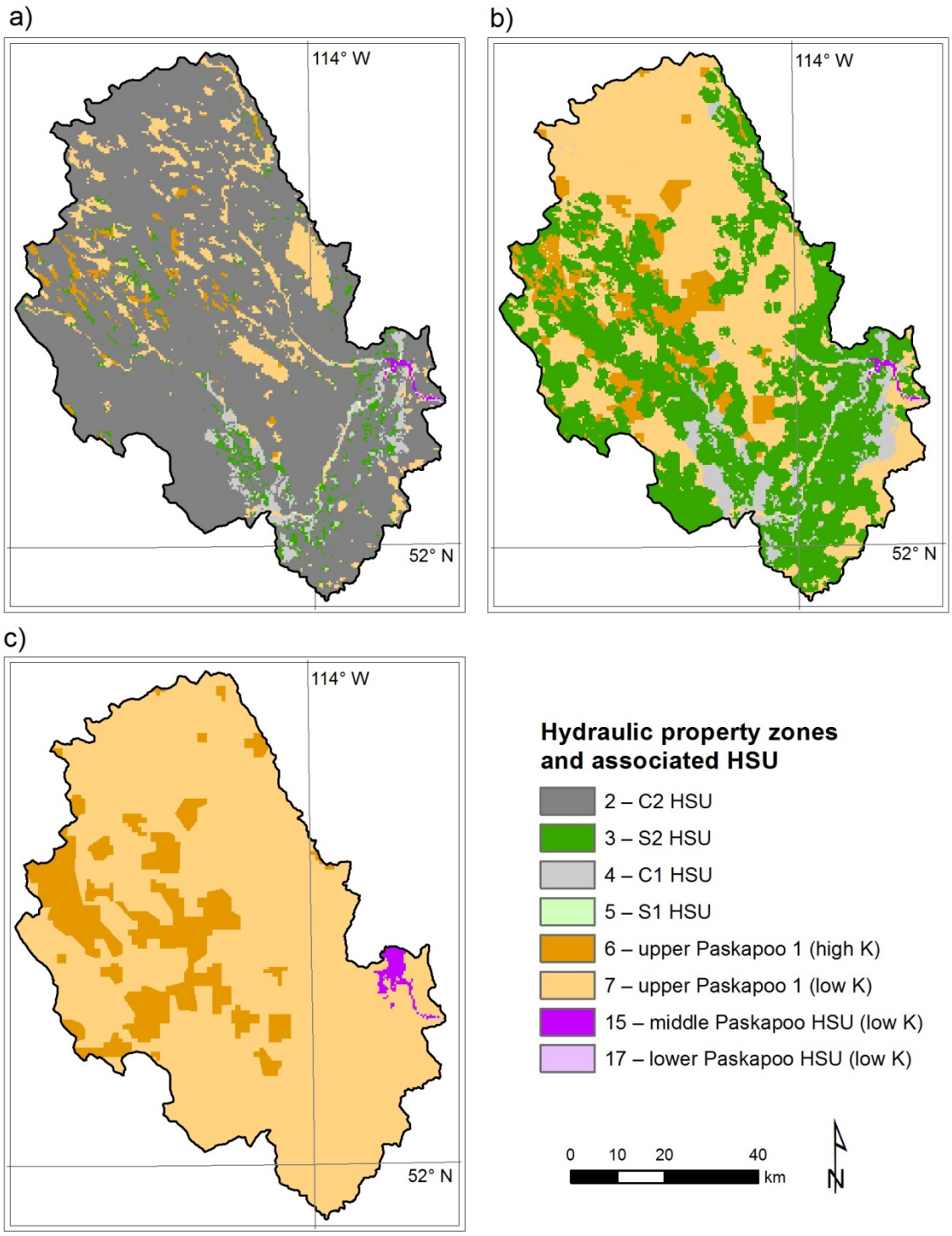

Figure 8. Hydraulic property zones in a) model layer 1, which is representative of C2 hydrostratigraphic unit (HSU); b) model layer 2, which is representative of S2 HSU; and c) model layer 5, which is representative of the topmost layer of the upper Paskapoo HSU (Sylvan Lake sub-basin, central Alberta). Where a particular HSU is absent, the grid cell is assigned a minimum thickness of 0.1 m and given the hydraulic properties of the HSU below. Abbreviation: K, conductivity.

3.3 Boundary Conditions

The conceptual and numerical models incorporate the influence of surface watershed boundaries on the local groundwater system in the upper layers of the model, and of regional flow boundaries in the deeper part of the system. No-flow boundaries were applied to the perimeter of the N–Q sediments and upper Paskapoo HSU layers, following the surface boundary of the Medicine–Blindman subwatershed (shallow domain; Figure 9). The lower Paskapoo HSU and deeper layers have specified head boundaries along the southwestern and northeastern portions of the domain, and no-flow boundaries along the northwestern and southeastern boundaries (Figure 9). The specified head boundaries are reflective of equipotential lines determined from the regional model by Singh et al. (2014) and allow for deep regional groundwater movement in a northeasterly direction throughout the model domain. Results of the regional model indicated very little difference in hydraulic head between the Paskapoo (modelled as one layer), Scollard, Battle, and Wapiti HSUs near the boundary areas; therefore, a specified hydraulic head value of 980 m was assigned to the southwestern boundary and 820 m to the northeastern boundary for all model layers within the deep domain.

The middle Paskapoo HSU is a combination of the two domains, with the active model extent and specified head boundary equivalent to the deep domain on the northern, southern, and western portions and a no-flow boundary at the northeastern edge, which follows the shallow domain boundary. This hybrid domain is used in order to reflect the eastwards shallowing and thinning of the middle Paskapoo HSU.

3.4 Model Stresses

Model stresses represent processes that add or remove water from a model domain. Stresses can be natural as well as anthropogenic. The stresses implemented in this model included recharge, rivers and lakes, and groundwater withdrawals (transient version only).

3.4.1 Steady-State Model

The steady-state model was developed in order to represent an average, long-term, hydrological condition in the SLSB. No pumping of groundwater was considered, and thus the steady-state scenario is seen as representative of average conditions. Figure 10 shows the recharge, rivers, and lakes that were implemented in the steady-state SLSB model.

3.4.1.1 Recharge

Net groundwater recharge (precipitation minus evapotranspiration and surface runoff) is input into the uppermost active layer of the numerical model. Twelve recharge zones (Figure 10, numbered 2–13) were implemented based on the northwest to southeast gradient in precipitation minus potential evapotranspiration. The recharge zones, not surprisingly, also follow regional changes in topography and land cover.

Recharge zones falling within the shallow domain boundary were initially assigned recharge values ranging between 10 and 60 mm/yr, which are within the range of previously identified recharge values for the Canadian Prairies (e.g., van der Kamp and Hayashi, 1998; Barker et al., 2011). Zones outside the shallow domain were assigned much lower recharge values, initially ranging between 1 and 7 mm/yr. Lower values are required in these areas because recharge is applied to the uppermost active layer, which is either the middle or lower Paskapoo HSU in the areas outside the shallow domain; therefore, recharge values are reflective of deeper recharge into the regional groundwater flow system. The recharge values were adjusted during the manual calibration stage in order to arrive at values of 35 mm/yr (zones 9, 12, 13; Figure 10) and 40 mm/yr (zones 8, 10, 11; Figure 10) within the shallow domain and 5 mm/yr (zones 2, 4–6; Figure 10) or 7 mm/yr (zones 3, 7; Figure 10) for zones within the deep domain. These values were fixed for the automatic calibration stages (Section 4).

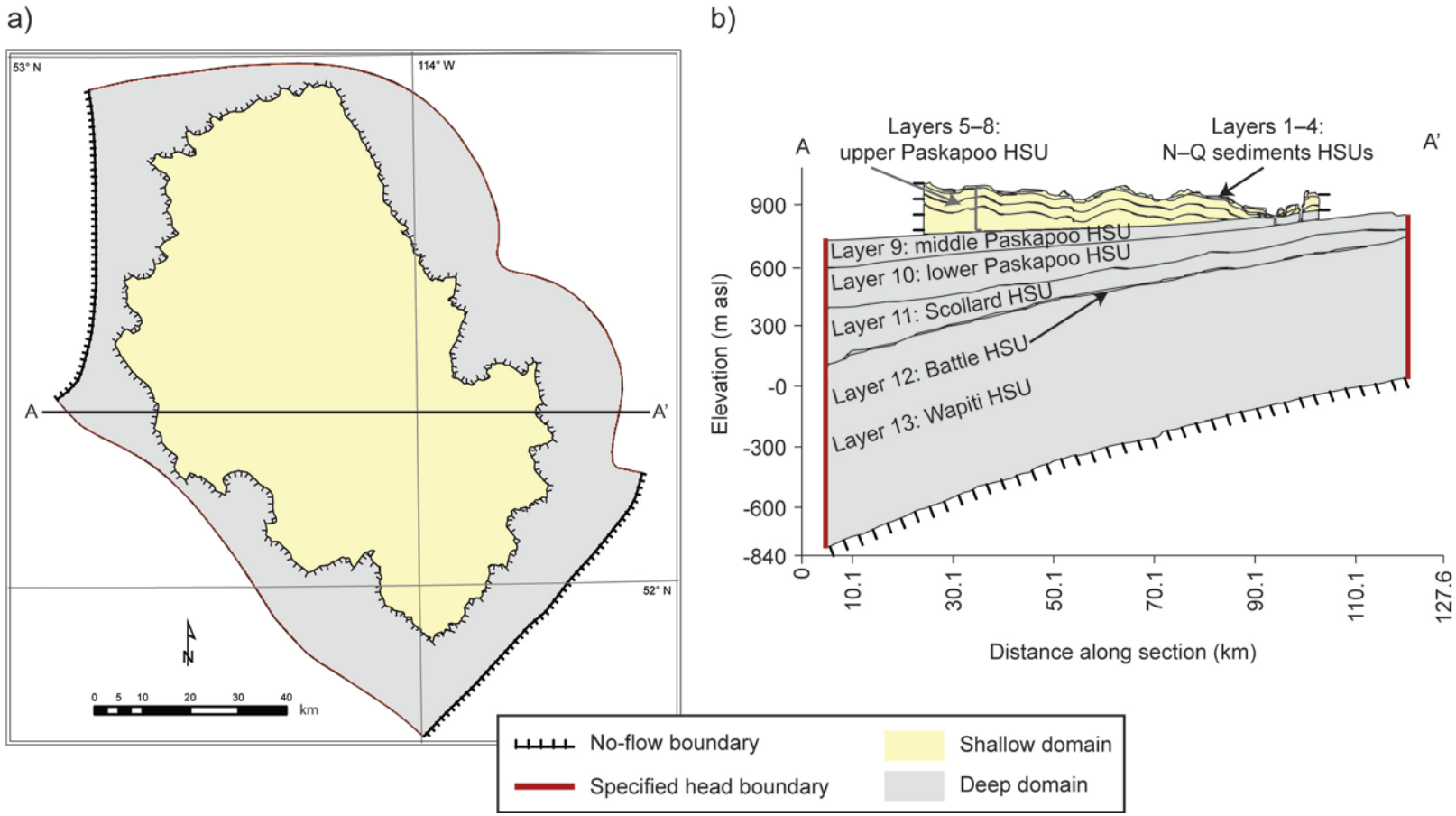

Figure 9. Boundary conditions for the Sylvan Lake sub-basin (SLSB), central Alberta, numerical model: a) plan view and b) cross-section of SLSB showing shallow and deep domains with associated no-flow and specified head boundary conditions. Abbreviation: HSU, hydrostratigraphic unit.

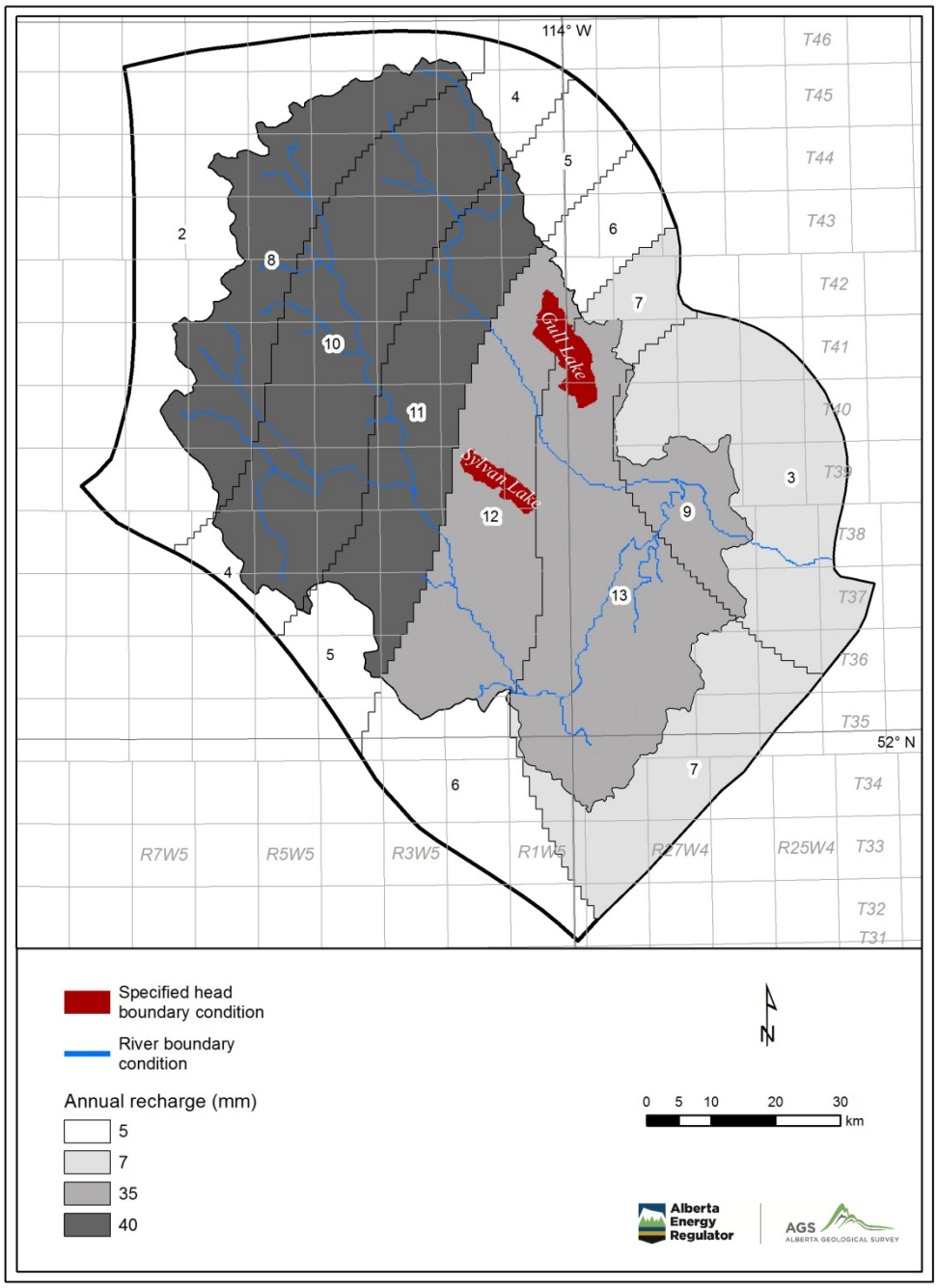

Figure 10. Steady-state model stresses for the Sylvan Lake sub-basin, central Alberta, numerical model. Numbers 2 to 13 correspond to model recharge zones, which are coloured according to the annual recharge (mm) used in the steady-state numerical model. Recharge zones 0 and 1 refer to inactive cells outside the deep domain and the lakes, respectively. Sylvan and Gull lakes are both simulated as specified head cells in the steady-state version of the numerical model.

3.4.1.2 Rivers and Lakes

Perennial streams and rivers within the SLSB were included in the numerical model with the MODFLOW river (RIV) package (Harbaugh et al., 2000; Figure 10), as the perennial characteristic of these features likely indicates a year-round connection to groundwater.

The river network used in the numerical model was extracted from a 25 m digital elevation model (DEM; Alberta Environment and Parks, 2015d), guided by 1:20 000 river linework (Alberta Environment and Parks, 2015b). Due to a lack of data on actual river bottom elevations and river stage, the river bottom elevation was generally set at 2.4 m below the elevation of the DEM for major streams, and 1 m below the ground surface for minor streams. The river stage was set as equal to the DEM surface, equivalent to a river stage of 2.4 m for major streams and 1 m for minor streams. Because of the unavailability of measured streambed conductance values for the river beds a uniform value of 1000 m/day (d) was assigned to all rivers based on the results of the manual calibration stage of numerical modelling (tested within a range of 10 to 10 000 m/d). The river conductance values were fixed for the remainder of the (automatic) calibration stages.

Sylvan and Gull lakes are the only surface water bodies simulated in the model. For the steady-state model, the lakes are simulated as specified heads. Sylvan and Gull lakes were assigned specified heads of 899 and 936.5 m asl, respectively, based on the average lake levels calculated from the HYDAT data.

3.4.2 Transient Model

A transient groundwater model was developed to account for responses to the time-variant stresses on the system. In the transient SLSB model, natural stress arises from variations in net recharge. The lake level and river inflows and outflows are allowed to vary in response to groundwater–surface water interaction. Anthropogenic stresses come from groundwater withdrawals due to pumping. The transient model is simulated and calibrated over the time period from January 1, 1995 to December 31, 1999. The transient model was run on monthly time steps and the simulated steady-state hydraulic head distribution served as the initial condition for all the transient simulations.

3.4.2.1 Recharge

As the calibrated steady-state model results showed little spatial variation in recharge, only two recharge zones were implemented in the transient model: one within the shallow domain (zones 8–13, Figure 10) and one for the areas outside the shallow domain but within the extent of the deep domain (zones 2–7, Figure 10). Monthly values of net recharge were applied uniformly across each zone and estimated based on the results of the steady-state model. For the area within the shallow domain, the monthly recharge rate was calculated as 8.4% of monthly precipitation, recorded at the Red Deer climate station (weather station Red Deer A; Alberta Agriculture and Forestry, 2014). This percentage is based on 40 mm/yr of recharge (from the range of 35–40 mm/yr of recharge determined from the steady-state model) as a percentage of annual precipitation at the Red Deer climate station (477 mm/yr from January 1963 to March 2014). For the area outside the shallow domain, where recharge is applied directly into the uppermost bedrock layer, 1.25% of monthly precipitation from the Red Deer climate station was input as net recharge into the model, based on the results of the steady-state modelling. In order to account for snowfall and frozen ground in the winter months, monthly recharge from November to March was summed and applied in April, when input from snowmelt would typically contribute to recharge. Annualized values of the recharge values input into the transient model range between 36 and 43 mm/yr for 1995 to 1998 and 55 mm/yr for 1999, which was a particularly wet year.

3.4.2.2 Rivers and Lakes

As with the steady-state model, the transient model simulates the rivers using the RIV package, with the same input parameters for conductance and river stage (Section 3.4.1.2). The river stages were held constant throughout the entire year at 2.4 m for major streams and 1 m for minor streams.

Sylvan and Gull lakes were simulated using the MODFLOW lake (LAK3) package (Merritt and Konikow, 2000), with a lakebed conductance value of 0.01 m/d. During the transient model manual calibration, it was determined that net precipitation into the lake was needed in order to simulate the seasonal variation of lake level. Therefore net precipitation equal to the net recharge rate discussed in Section 3.4.1.2 was applied to both lakes. This provides a large influx to the lakes in the spring, when

snowmelt and surface runoff are occurring, and a smaller to no influx over the fall and winter. In reality, there is a highly transient interplay between precipitation onto the lake and evaporation out of the lake, which was not accounted for in this version of the model.

3.4.2.3 Groundwater Withdrawal

Groundwater is withdrawn from the SLSB due to pumping for domestic, agricultural, municipal, and industrial purposes. Domestic and traditional agricultural users are permitted to pump a maximum of 1250 or 6250 m^3 of groundwater per year, respectively, without a licence. There is no required monitoring for these unlicenced wells, therefore there is no information in the AWWID on how much water is actually pumped in a given year, or if a well is actively in use (unless it is marked as 'reclaimed' in the AWWID). Additionally, return flow from domestic septic fields in the vicinity of domestic groundwater users has not been quantified. Due to the uncertainty about actual net groundwater withdrawals, unlicenced wells are not included in the transient simulation. Indeed, the effects of a widespread groundwater sink such as that which may be created by unlicenced wells may also be offset in the model simulation by an increase in recharge to the system, whilst maintaining the same set of calibration parameters.

Licenced water wells are allocated a maximum amount of annual groundwater withdrawal. In some cases, information on actual volumes, pumping rates, or water levels are available for a particular well, although these were not considered in this study. Licenced water well data were obtained from AEP for the SLSB area and queried to extract wells with location, production depth, and maximum annual diversion volume information. Daily pumping rate (m^3/d) was determined by dividing the maximum annual diversion volume by 365 days. Approximately 900 water wells were selected to include in the transient simulation (Figure 11). For the current model version, wells with a pumping rate of less than 0.6 m^3/d or a depth of less than 5 m were neglected. The extraction rate for a particular well was divided between multiple model layers if necessary in accordance with the screened interval.

4 Model Calibration and Evaluation

Model calibration and evaluation was performed using the entire extent of the model; however, the results within the areal extent of the shallow domain are of most interest in this study. The larger extent of the deep domain provides a buffer between the regional constant head boundaries and the main area of interest within the areal extent of the shallow domain and it is expected that there are some model edge effects in this area.

The calibration approach implemented for the model included both manual and automatic methods. The objective of the automatic calibration is to minimize the sum of squared errors (SSE) between measured and simulated groundwater hydraulic heads at selected calibration points, according to:

$$SSE = \sum_i^n \left(H_{observed_i} - H_{simulated_i}\right)^2 \qquad (1)$$

where n is the number of calibration targets, $H_{observed}$ and $H_{simulated}$ are observed and simulated hydraulic heads, respectively, at a given calibration point i. Calibration of the steady-state model involved automated hydraulic conductivity adjustment within upper and lower limits to obtain an optimal solution. The upper and lower limits for the calibration were set as one order of magnitude above and below field measured and literature values (Table 2). Considering the objective and spatial scale of the numerical model, no attempt was made during the automated calibration to modify the conductance values of the riverbeds and lakebeds. Instead, model results from the rivers and lakes were used to validate the results of the simulations by comparison to observed data. The dynamically dimensioned search (DDS) algorithm, developed by Tolson and Shoemaker (2007), was used for calibration. Parameter values from the steady-state calibration were then used in the transient model with some manual calibration of other parameters such as specific yield, lakebed conductance, and direct precipitation onto the lake.

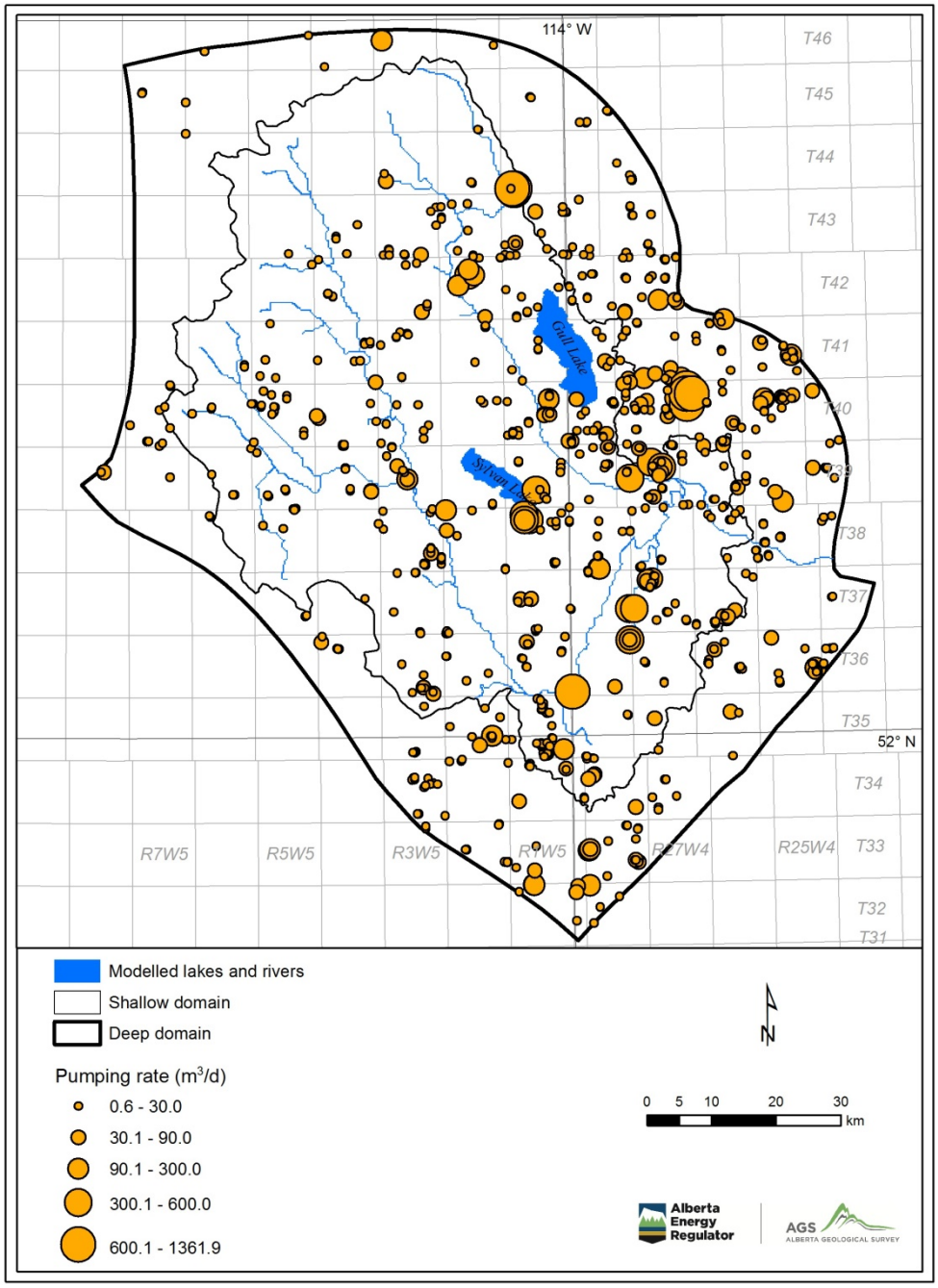

Figure 11. Licenced water well pumping rates, Sylvan Lake sub-basin, central Alberta. Abbreviation: d, day.

4.1 Steady-State Model

Calibration of the steady-state model attempts to simulate the long-term average conditions of the SLSB. Figure 12 shows the location of water level data from water wells used as calibration targets and observation points. Water level data were extracted from the AWWID and the Groundwater Observation Well Network (GOWN; Alberta Environment and Parks, 2015c). The AWWID contains 26 000 wells in the deep domain area with water-level information, with records spanning 90 years from 1925 to 2015. In

order to reduce the number of calibration targets and constrain the steady-state calibration to more recent average conditions, 447 wells from the AWWID were selected based on following criteria:

- wells with only one well record, one screened interval, and one recorded static water level;
- wells drilled after January 1, 2005 (according to drill end date); and
- only one well per quarter township, per geological unit; if there were multiple wells per quarter township, the most recent well was selected.

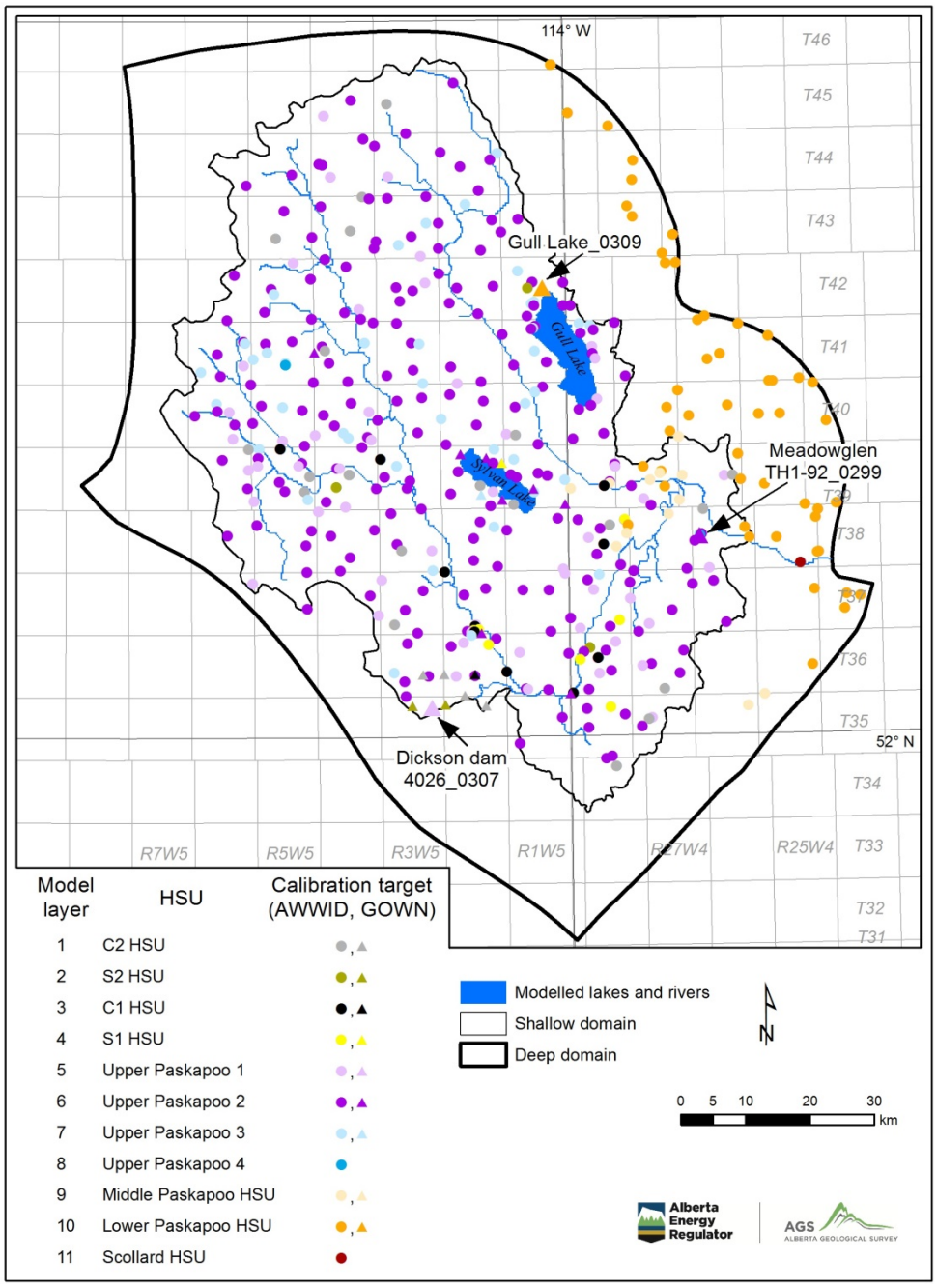

Figure 12. Steady-state calibration targets for the Sylvan Lake sub-basin, central Alberta. The three labelled Groundwater Observation Well Network (GOWN) wells are also used as observation points in the transient model. Abbreviations: AWWID, Alberta Water Well Information Database; HSU, hydrostratigraphic unit.

The hydraulic head (i.e., calibration target) for each AWWID well was determined by subtracting the recorded static water level from the ground surface elevation from the DEM (25 m cell; Alberta Environment and Parks, 2015d) at that location, as there is limited data within the AWWID on surface or top of casing elevation.

Thirty wells from the GOWN network were selected as calibration targets based on the availability of data such as screen interval, lithology, water level record, and the location of the well in relation to nearby GOWN wells. The hydraulic head (i.e., calibration target) for each well was calculated using the average hydraulic head from the monitoring record.

Finally, average water level data from 10 shallow wells monitored by Alberta Agriculture and Forestry for water quality management purposes were also used as calibration targets, however, these wells are not shown in figures or in available data due to confidentiality reasons.

The calibrated steady-state model has an SSE of 1.2×10^5 m^2. The results of the calibrated steady-state numerical model of hydraulic head were evaluated quantitatively to check for any systematic bias in the results. Figure 13 shows a histogram of the residual values (i.e., difference between simulated and observed hydraulic heads) and the normal probability plot of the residuals. An Anderson Darling normality test (Anderson and Darling, 1954) fails to reject the null hypothesis, at the 5% significance level with a p-value of 10.8%, indicating that the residuals are normally distributed. The histogram and the probability plot also support the normality test (i.e., the residuals are normally distributed).

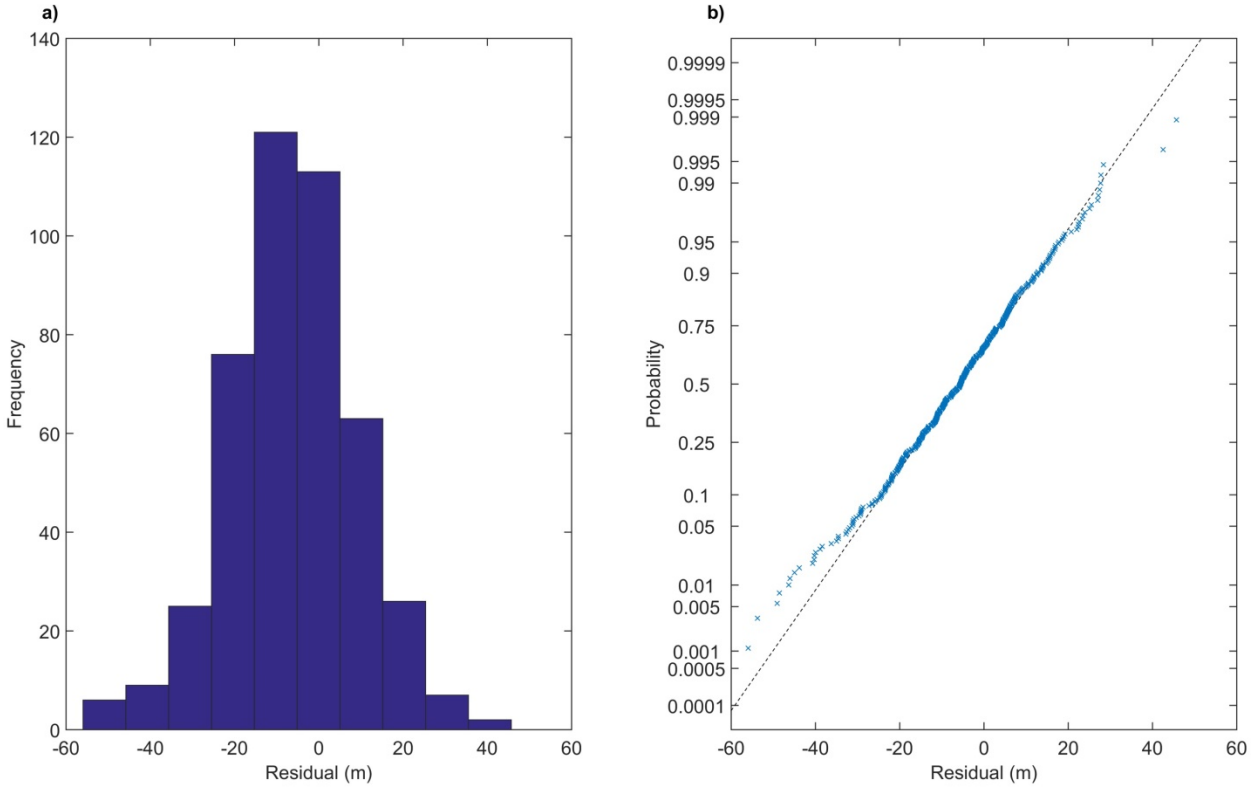

Figure 13. Calibrated steady-state model evaluation for hydraulic head, Sylvan Lake sub-basin, central Alberta: a) histogram of residuals (difference between simulated and observed hydraulic heads), and b) normal probability plot for residuals.

Figure 14 shows the cross-validation plot between simulated and observed hydraulic heads in various layers in the steady-state model along with the R^2 values, which is a statistical measure of how closely the data fits a linear regression line. The R^2 value of all the calibration targets together is 0.95. Figures 13 and 14 show a slight underestimation of observed hydraulic head in the simulation.

Figure 15 shows the spatial distribution of residuals in the study domain. There is no strong spatial bias of residuals although the model slightly underestimates hydraulic head in elevated areas and slightly overestimates hydraulic head along the low-lying river valleys. The statistical measurements and the water level comparisons show that the calibrated steady-state hydraulic head solution reasonably matches the water levels in the target wells.

The sensitivity of the calibrated steady-state model to hydraulic conductivity was evaluated. Each hydraulic conductivity parameter was adjusted while all other parameters were kept at the calibrated values. The hydraulic conductivities were increased and decreased by an order of magnitude (0.1 to 10 times the calibrated value). The sensitivity of the model was evaluated by the corresponding change in magnitude of the calculated SSE values (Equation 1). Figure 16 shows a summary of the results from the sensitivity analysis. The model shows more sensitivity to changes in the horizontal hydraulic conductivities as compared to the vertical conductivities. Additionally, the model shows the most sensitivity to changes in hydraulic conductivity in the upper Paskapoo 2 model layer. The model shows much lower sensitivity to hydraulic conductivities in the Scollard, Battle, and Wapiti HSUs, although this may be attributed to their depth and a lack of observation wells in these formations.

Following the calibration, the steady-state model was evaluated based on a comparison to observed river flow data from the HYDAT database. Using the incremental drainage areas shown in Figure 3, each area was assigned an individual zone within the ZONEBUDGET package (Harbaugh, 1990) to assess the water budget within each area, including groundwater contribution to river flow. However, only three gauges operate continuously throughout the year in the study area (stations 05CC001, 05CC002, 05CC007; Figure 3), hence the simulated groundwater contributions to rivers were summed for all zones contributing to each of the three continuous gauging stations.

In order to estimate actual groundwater contribution to river flow, the average daily volumetric flow rate from each of the three continuous gauging stations was calculated from measurements collected in the winter months only (November 1st to February 29th), when groundwater discharge is likely the main contributor to river flow rather than surface runoff or subsurface stormflow. The estimated observed contribution of groundwater to river flow was compared to the simulated net flow rate of groundwater out of the subsurface into the river cells. The results obtained from the model are in good agreement with those estimated from the gauging stations (Table 3). It is noted that whereas the Medicine and Blindman rivers (measured at stations 05CC007 and 05CC001, respectively) receive no river flow from outside the SLSB (i.e., the headwaters are within the SLSB), the Red Deer River (measured at station 05CC002) receives water from outside the SLSB and is controlled by the Dickson dam. The influence of the dam on the Red Deer River and its interactions with groundwater is not considered in this study.

Table 3. Average observed winter flow and simulated net groundwater output to rivers, Sylvan Lake sub-basin, central Alberta.

Station Number	Station Name	Average Observed Winter Flow (m^3/day)	Simulated Net Groundwater Output to Rivers (m^3/day)
05CC001	Blindman River near Blackfalds	3.8×10^4	3.2×10^4
05CC007	Medicine River at Eckville	4.5×10^4	3.8×10^4
05CC002	Red Deer River at Red Deer	1.2×10^6	1.2×10^5

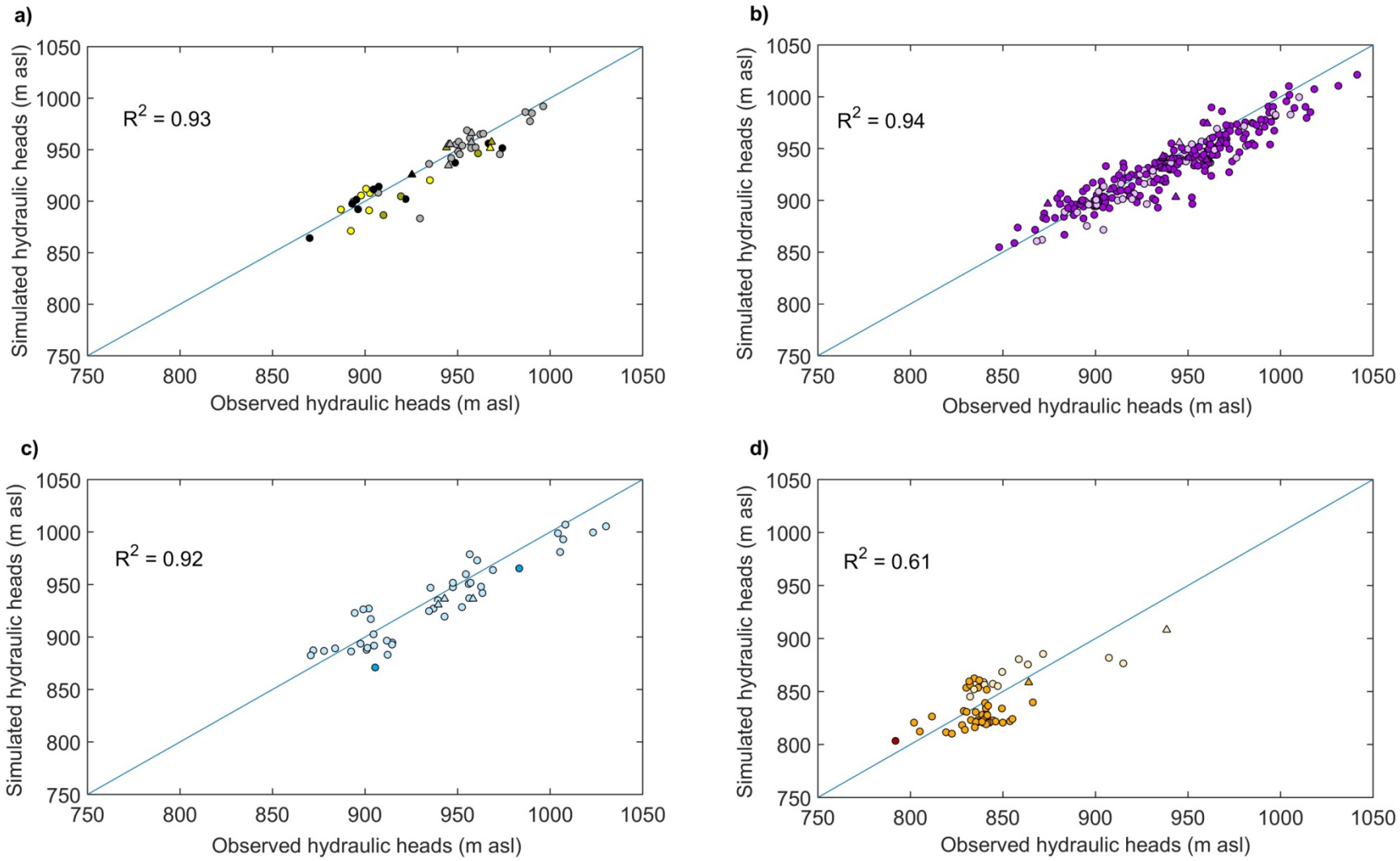

Figure 14. Cross-validation plots between the steady-state simulated hydraulic heads and the observed hydraulic heads from wells shown in Figure 12 (see Figure 12 for symbol legend), Sylvan Lake sub-basin, central Alberta: a) model layers 1–4 (generally Neogene–Quaternary [N–Q] sediments hydrostratigraphic units [HSUs]); b) model layers 5 and 6 (generally upper Paskapoo 1 and 2); c) model layers 7 and 8 (generally upper Paskapoo 3 and 4); and d) model layers 9–11 (generally middle Paskapoo, lower Paskapoo, and Scollard HSUs). Abbreviation: R, correlation coefficient.

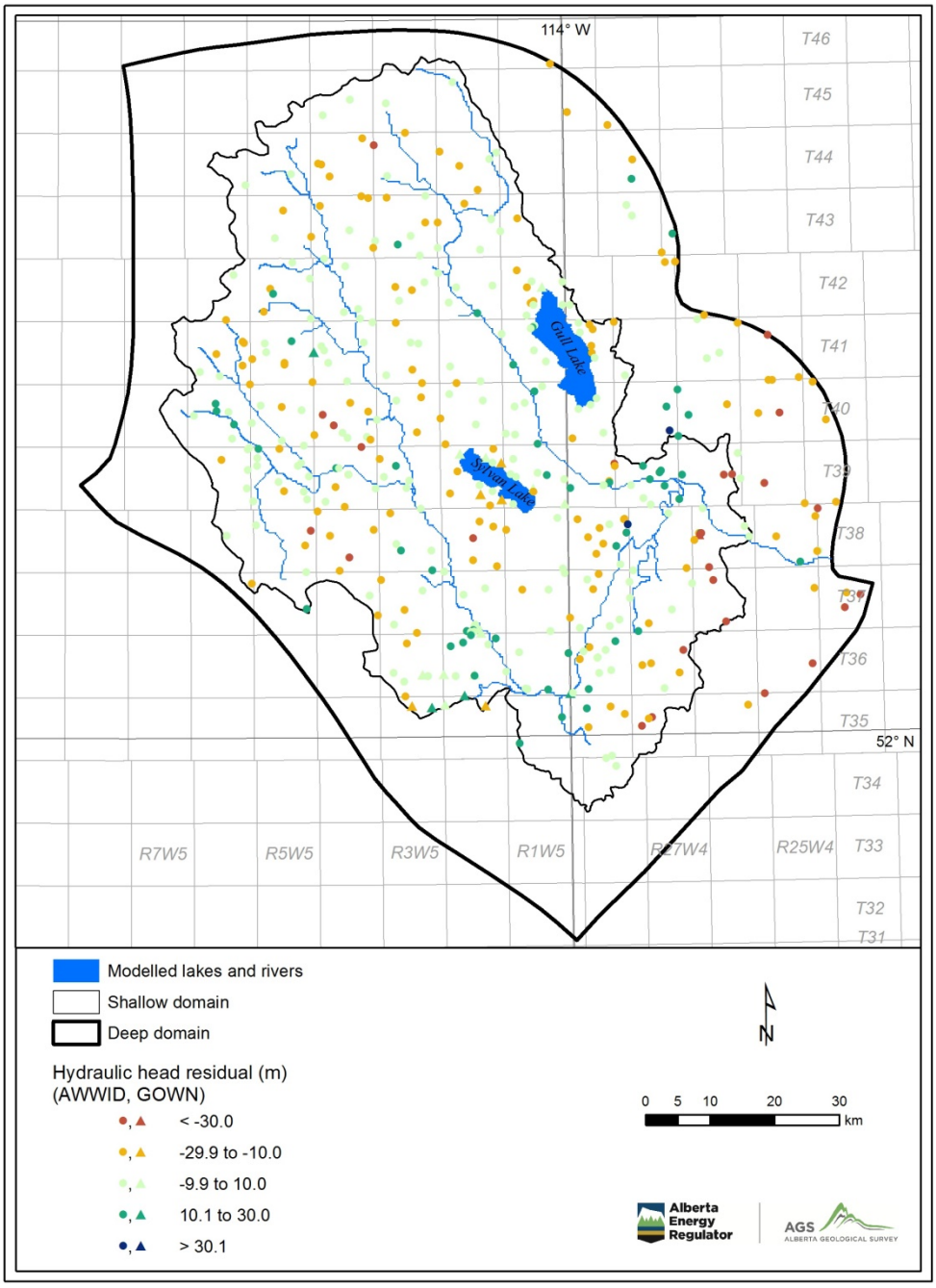

Figure 15. Spatial distribution of hydraulic head residuals in the steady-state model (simulated head minus observed head) of the Sylvan Lake sub-basin, central Alberta. Abbreviations: AWWID, Alberta Water Well Information Database; GOWN, Groundwater Observation Well Network.

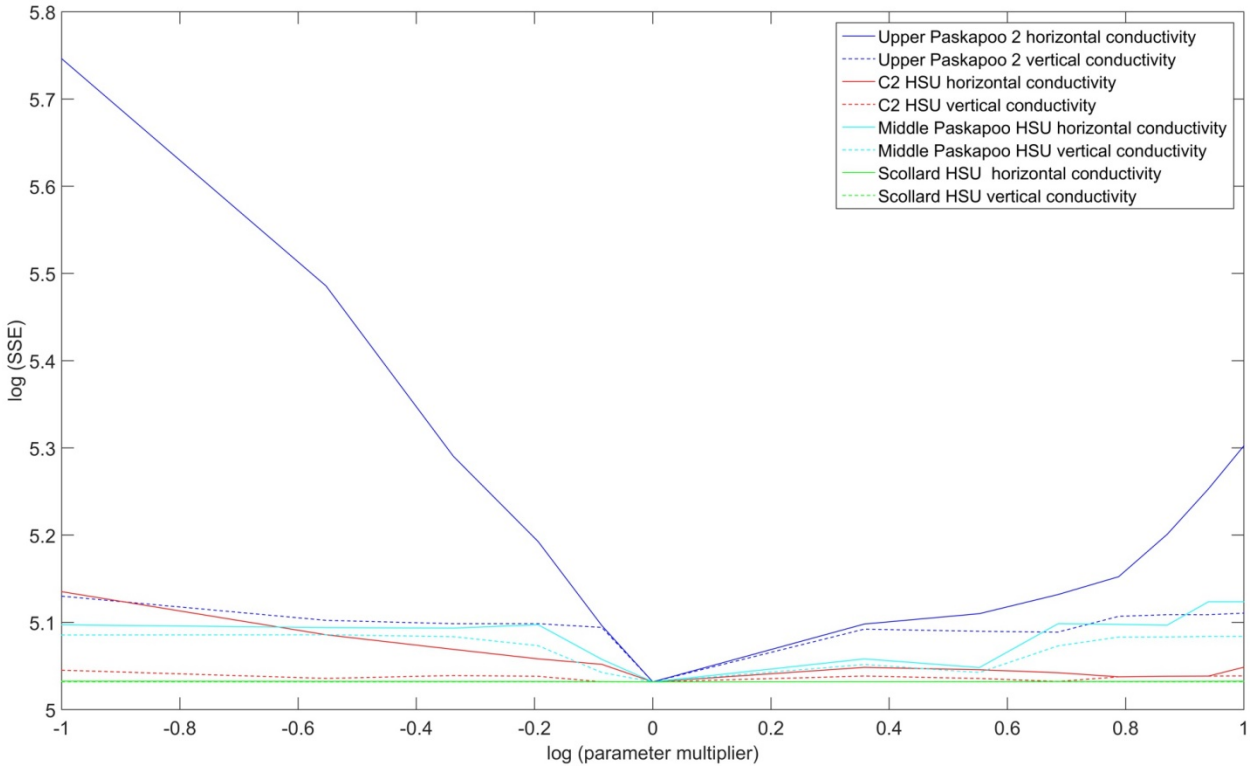

Figure 16. Summary of the results of the sensitivity analysis of calibrated steady-state model to hydraulic conductivity changes (Sylvan Lake sub-basin, central Alberta). Each line series shows the model sum of squared errors (SSE) for a given multiplier (x-axis) of the parameter specified in the legend. Abbreviation: log, logarithm.

4.2 Transient Model

The transient groundwater flow model provides an opportunity to evaluate the relationship between transient stresses and temporal changes in the water table and groundwater flow directions. The SLSB lacks a robust amount of time-variant data that is both spatially distributed and temporally coincident. This lack of data imposes a limitation on the model results in terms of bias towards the location of data availability. Because of this lack of data, the transient model was not automatically calibrated as was done with the steady-state model; however, a couple parameters such as specific yield were manually calibrated. Figure 12 shows the three GOWN wells and the two lakes used as observation points for the transient model simulation period from January 1, 1995 to December 31, 1999. None of the wells have continuous data measurements over the calibration period.

Figure 17 shows the observed and simulated hydraulic heads for three GOWN wells for the simulation period. The recorded depths to water for each GOWN well were subtracted from the model surface in order to compare the observed and simulated hydraulic heads. The Meadowglen TH1-92_0299 well (Figure 17a) shows the greatest difference between observed and simulated hydraulic head, whereas the Gull Lake_0309 well shows the least difference. Some difference in hydraulic head is expected given the regional nature of the numerical model and the averaging of simulated hydraulic head over a 200 m grid cell. The seasonal variation in head (or lack of in the case of Meadowglen TH1-92_0299 well) is well captured. It is also noted that Meadowglen TH1-92_0299 and Gull Lake_0309 wells are affected by human activity. The observed well data at only three points highlight the lack of transient calibration data in the sub-basin.

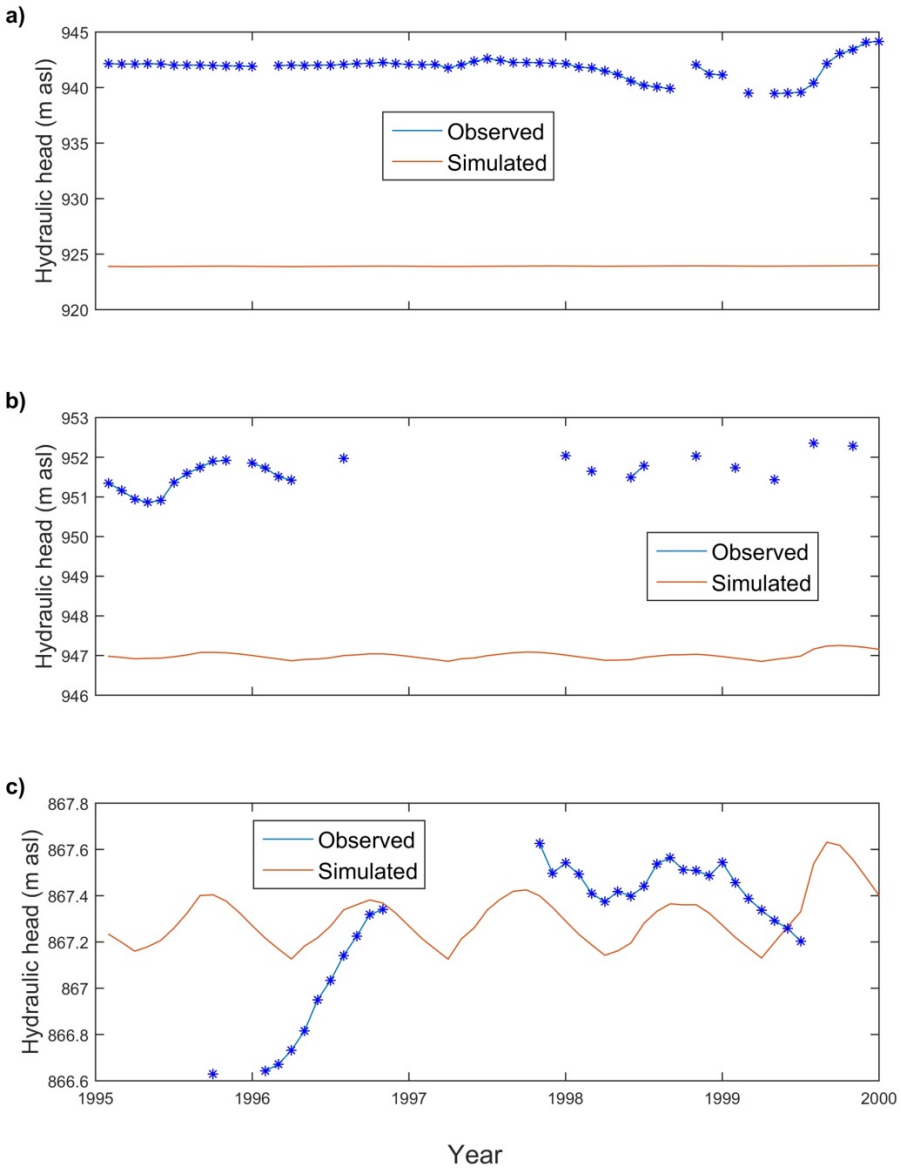

Figure 17. Simulated versus observed hydraulic head in three Groundwater Observation Well Network (GOWN) wells, Sylvan Lake sub-basin, central Alberta: a) Meadowglen TH1-92_0299, b) Dickson Dam 4026_0307, c) Gull Lake_0309. Location of wells is shown on Figure 12.

Figure 18 shows the simulated lake level along with the average monthly observed lake level for both Sylvan and Gull lakes. The observed lake levels for both lakes are relatively constant throughout the year, varying only by approximately 30 cm throughout the five-year simulation period. The simulated lake levels lie within the range of observed levels; however, they do not have the same amplitude of seasonal variation. There is also a trend of increasing lake levels in the simulation. This trend is due partly to an increasing trend in precipitation throughout the five-year simulation period, although it is likely that an absence of detailed monthly precipitation to and evaporation from the lake in the numerical model may also contribute. Baker (2009) determined a net loss from Sylvan Lake due to evaporation, whereas the numerical model had a small net gain from precipitation. Results of the sensitivity analysis (results not shown) indicate that lakebed conductance has a small effect on lake level, but the trend remains the same. Lake levels in the numerical simulation are controlled primarily by the surrounding hydraulic heads and precipitation.

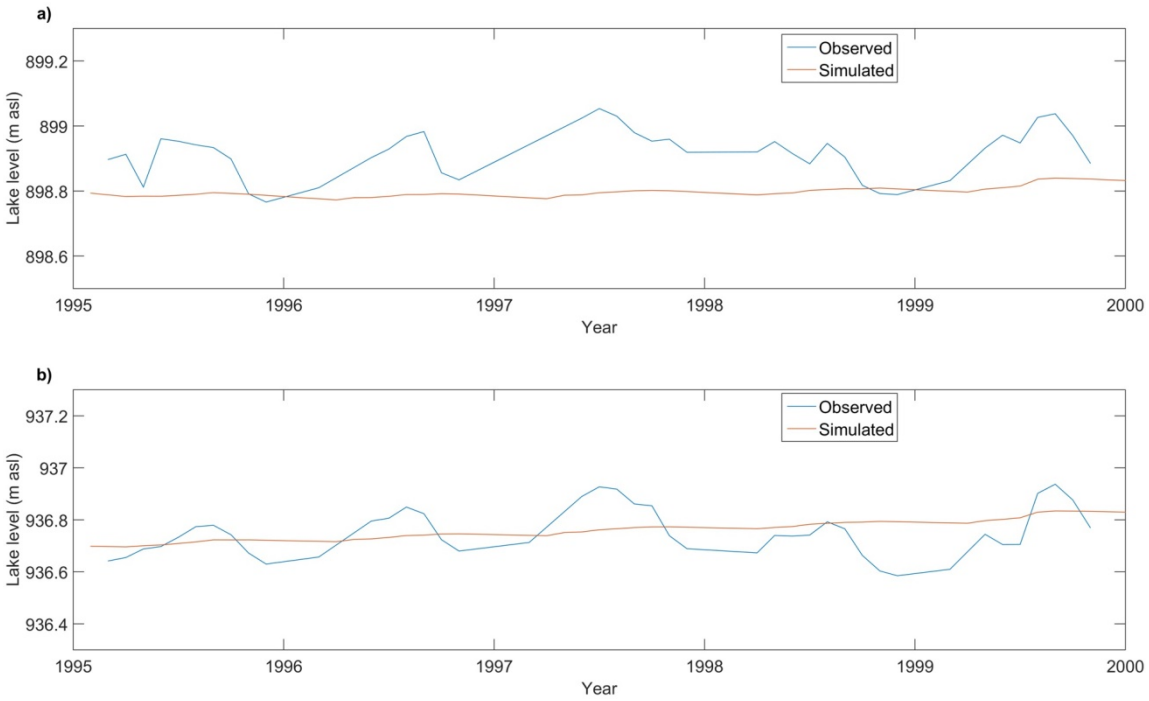

Figure 18. Simulated versus observed lake level in a) Gull Lake and b) Sylvan Lake, Sylvan Lake sub-basin, central Alberta.

Overall, the results of the transient simulation are adequate for the purpose of an initial capture of groundwater movement in the SLSB. Improvements to the model could be made following the suggestions in Section 6.

The sensitivity of the transient model was determined by evaluating the results of the following scenarios, for a total of 13 additional simulations from the base case:

- no groundwater pumping;
- recharge doubled and halved;
- lakebed conductance increased to 0.1 and 10 m/d;
- K_x and K_y doubled and halved. K_z was adjusted in order to maintain the same anisotropic ratio for each property zone (Table 2); the property zones were grouped as follows:
  - N–Q sediments HSUs,
  - upper Paskapoo HSU,
  - middle and lower Paskapoo HSUs, and
  - Scollard, Battle, and Wapiti HSUs.

Table 4 shows the impact of the sensitivity simulations on the net flux of water into the model as well as the changes in the water table from the base case. The fluxes in the transient model are most sensitive to changes in recharge and in the hydraulic conductivities of the Paskapoo HSUs, which is similar to the results found for the steady-state model. This is due to the direct connection of the Paskapoo HSUs with the two lakes and most of the rivers. Although Table 4 shows that there may be large local changes in the elevation of the water table (i.e., maximum increase and decrease of hydraulic head), there is very little change in the overall water table elevation (i.e., median change).

Table 4. Results of the sensitivity analysis of the transient model simulation, Sylvan Lake sub-basin, central Alberta. Shaded colours represent negative (more red) and positive (more blue) percent changes from the base case. Abbreviations: HSU, hydrostratigraphic unit; K_x, K_y, horizontal hydraulic conductivities; N–Q, Neogene–Quaternary.

Model Run		Change in Net Flux of Water from Base Case (%)			Change in November 1998 Water Table Elevation from Base Case (%)			Change in August 1999 Water Table Elevation from Base Case (%)		
		Constant Head Boundaries	River Leakage	Lake Seepage	Maximum Increase	Maximum Decrease	Median Change	Maximum Increase	Maximum Decrease	Median Change
Double recharge		-13.7	6.4	-15.5	0.8	-6.9	-0.03	6.7	-12.0	-0.02
Half recharge		7.0	-3.3	7.9	9.7	-1.3	0.05	15.2	-1.5	0.04
No pumping		-0.8	0.2	-1.1	3.2	-2.9	0.00	11.6	-9.7	0.00
N-Q sediments HSUs	Double K_x,K_y	0.0	0.2	0.1	2.7	-6.8	-0.01	4.3	-10.1	-0.01
	Half K_x,K_y	0.0	0.4	0.7	8.0	-4.6	0.01	15.2	-3.8	0.01
Upper Paskapoo HSU	Double K_x,K_y	11.0	-3.2	-35.0	5.3	-2.9	0.00	15.2	-2.7	0.00
	Half K_x,K_y	-13.7	5.9	41.9	2.8	-4.2	0.00	8.8	-12.8	0.00
Middle and lower Paskapoo HSUs	Double K_x,K_y	-39.7	-38.5	-1.2	13.3	-9.5	0.00	4.1	-4.4	0.00
	Half K_x,K_y	60.5	56.8	15.7	8.9	-8.4	0.00	5.3	-3.8	0.00
Scollard, Battle, and Wapiti HSUs	Double K_x,K_y	0.0	0.0	0.0	3.2	-3.0	0.00	10.7	-5.6	0.00
	Half K_x,K_y	0.0	0.0	0.0	3.2	-2.9	0.00	9.9	-7.1	0.00
Lakebed conductance values (m^3/day)	0.1 m/day	0.0	0.0	1.5	3.2	-2.3	0.00	10.4	-9.9	0.00
	10 m/day	-1.2	6.3	-18.3	6.5	-3.3	0.05	15.2	-9.9	0.06

Similar to the steady-state model, ZONEBUDGET was run on the transient model with zones aligned to the Agriculture and Agri-Food Canada incremental drainage areas (Figure 3). Figure 19 shows the mean monthly observed river flow at each of the three continuously measured HYDAT river gauging stations. Overlain are the results of the net groundwater to river flow from the incremental drainage areas contributing to the particular gauging station. The results show that groundwater discharge to rivers is lower than the low flow rate of the rivers during the winter months, and in the case of station 05CC007 there is some leakage from the rivers into the groundwater. Although the absolute amount of groundwater discharge to rivers may not be captured well by the model, the relative seasonal changes and response to precipitation is well-captured. It is noted that the observed river flows also include water that enters the river via overland flow and short-duration subsurface stormflow pathways, as such, the comparison with simulated groundwater discharge results is applied in a general sense.

5 Model Results

Model results include simulated steady-state hydraulic head, hydraulic head change in the period from 1995 to 1999, and simulated flows of water into and out of the model (water budget).

5.1 Groundwater Movement

5.1.1 Steady-State Model

Figure 20 presents the steady-state water table in the SLSB, along with a west to east cross-section. In general, the hydraulic head distribution shows that local- to medium-scale, topography-driven flow systems dominate. The flow paths are a subdued replica of the general topographic gradient of the land surface. Higher simulated hydraulic heads in the Paskapoo HSUs in the northern part of the domain correspond to the topographically high regions. The influence of the topographically low river systems on groundwater is highlighted in the trend of lower simulated hydraulic heads along the river valleys.

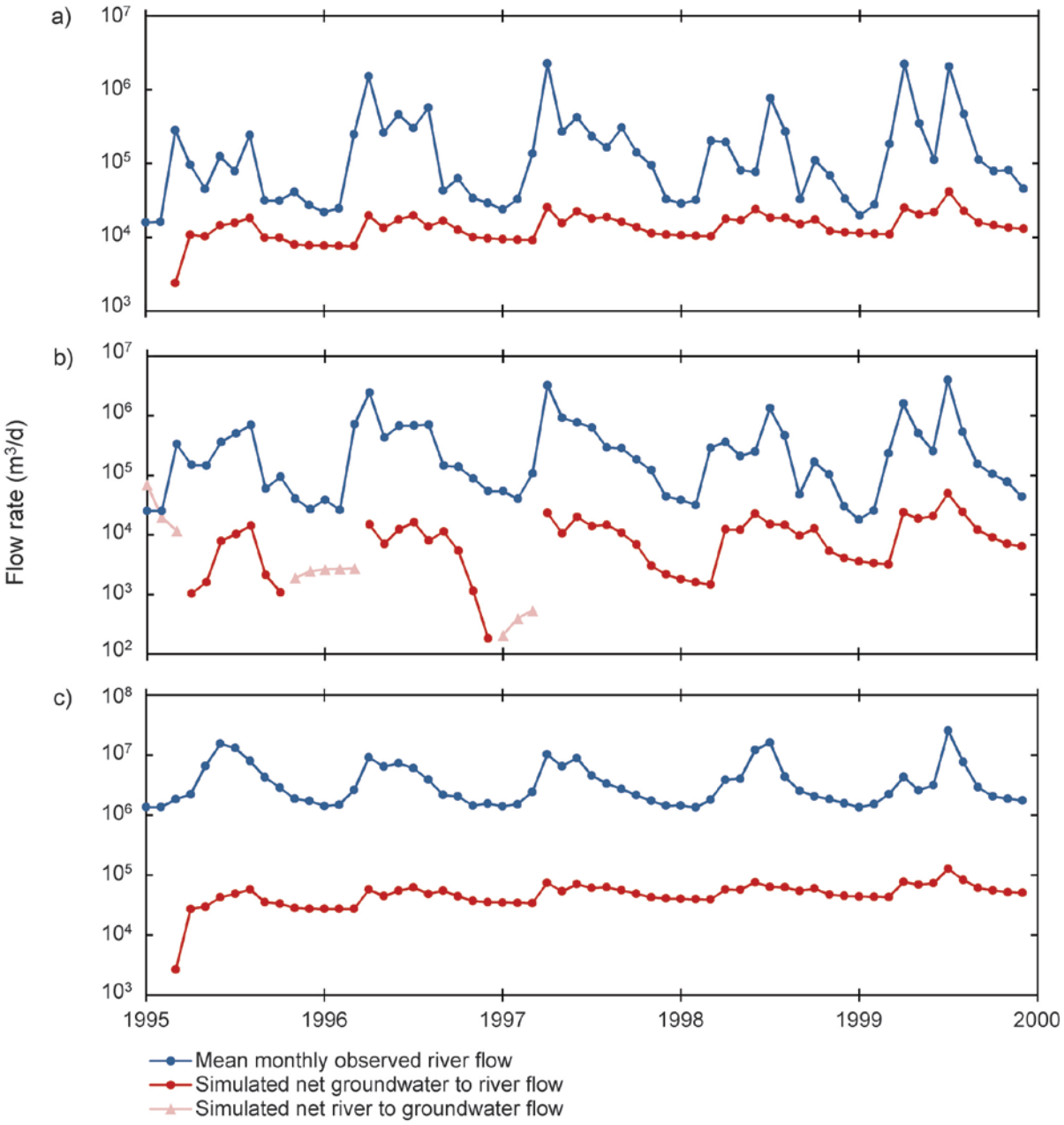

Figure 19. Simulated net flow of groundwater to rivers and vice versa compared to observed river flow at gauging stations a) 05CC001, b) 05CC007, and c) 05CC002, Sylvan Lake sub-basin, central Alberta. Simulated net flow is summed from all incremental drainage areas contributing to a particular gauging station (Figure 3). Abbreviation: d, day.

Figure 21 presents the hydraulic head difference between model layers 1 and 13, which represents the regional recharge potential based on the hydraulic heads in each respective unit. Figure 21 shows the highest regional recharge potential in the northwest whereas regional discharge potential occurs along the rivers. Figure 22 presents the vertical hydraulic head in each model layer along a cross-section in the SLSB. This figure highlights the fact that the recharge takes place along the topographically high regions and rivers act as groundwater discharge zones.

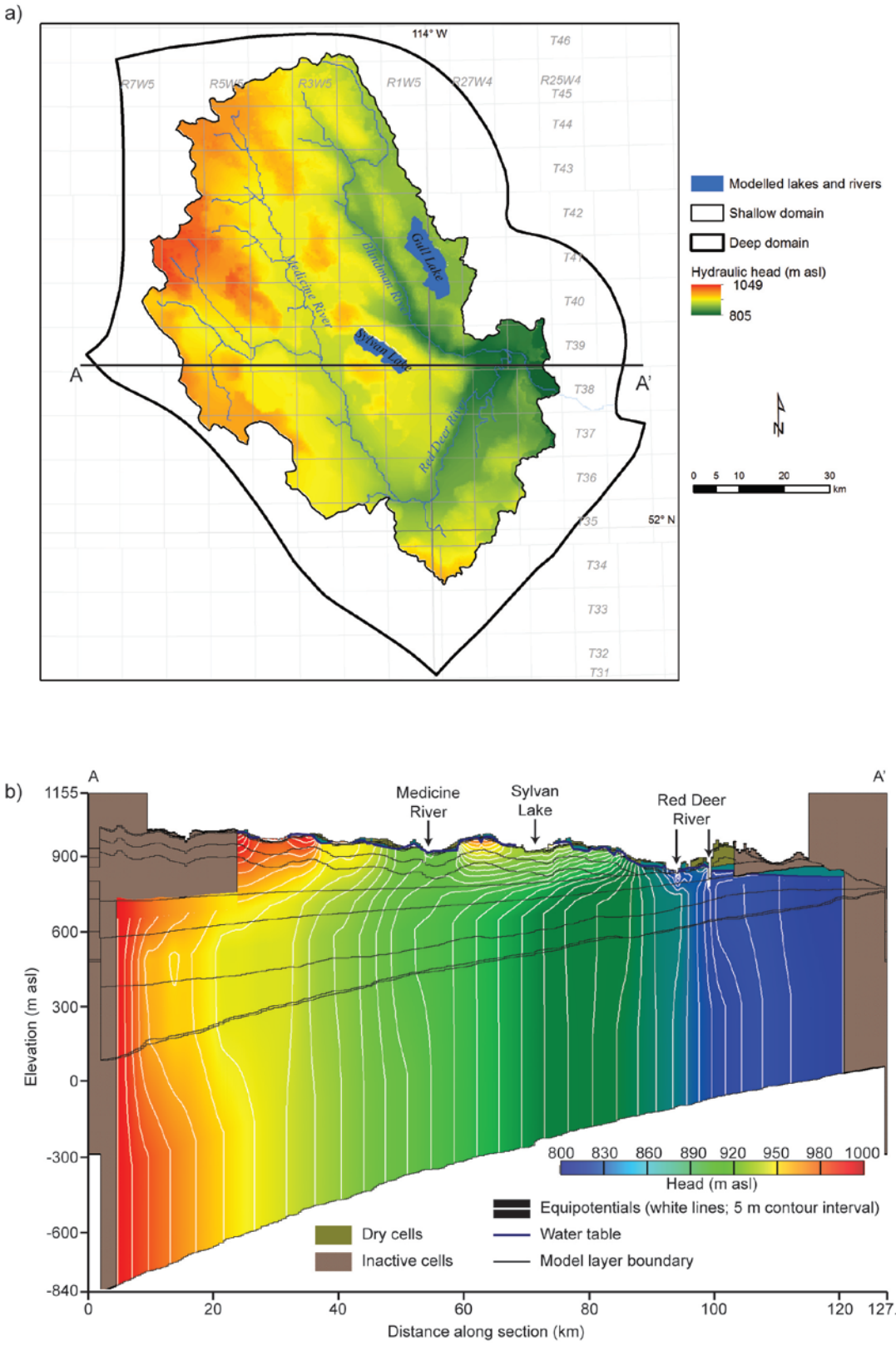

Figure 20. Steady-state hydraulic head distribution in the Sylvan Lake sub-basin, central Alberta: a) plan view of the hydraulic head distribution of the water table, and b) west to east cross-section showing vertical distribution of the hydraulic head.

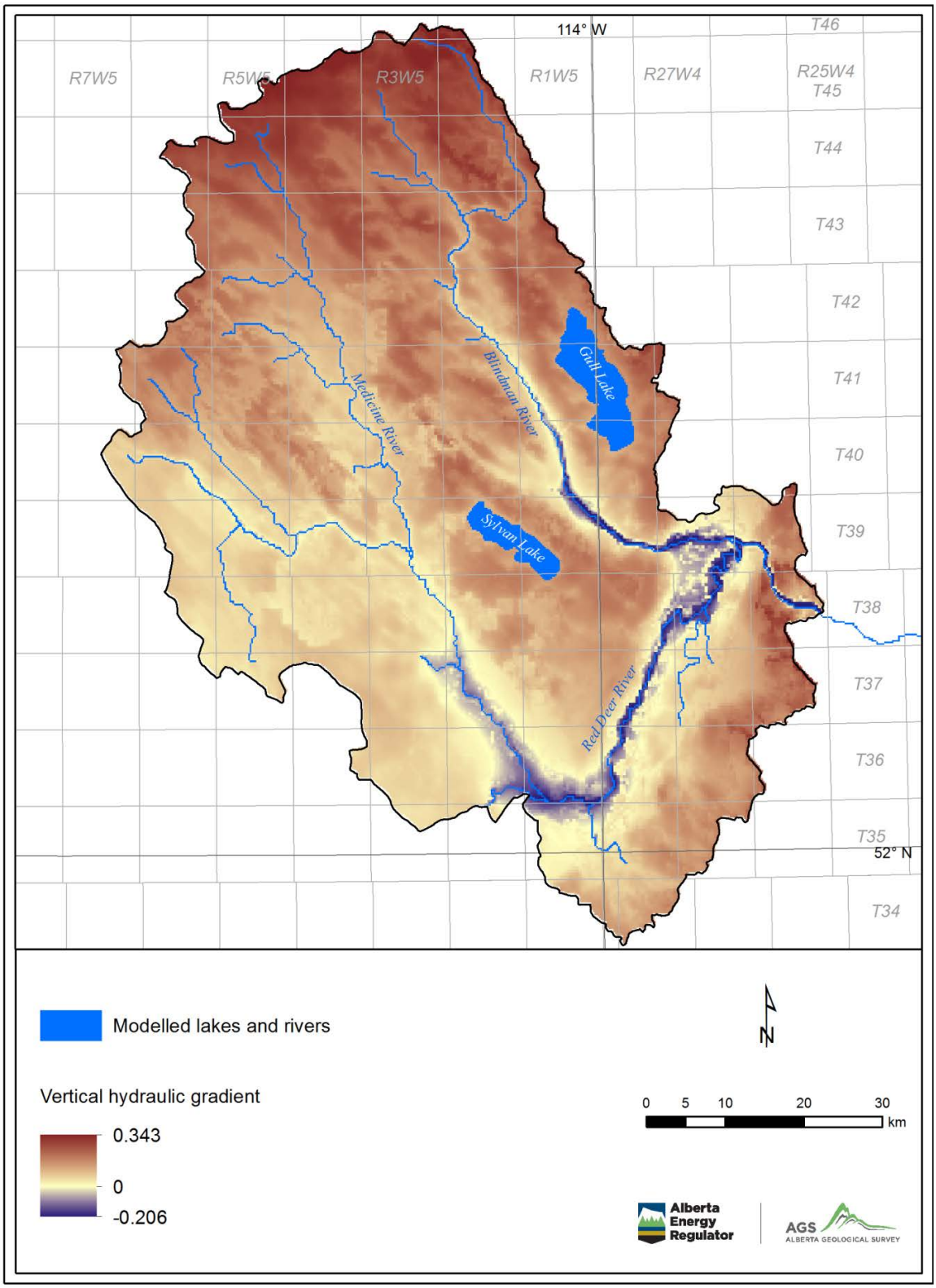

Figure 21. Recharge potential shown as the simulated vertical hydraulic gradient between model layers 1 and 13 (hydraulic head divided by thickness between layers 1 and 13), Sylvan Lake sub-basin, central Alberta. Negative values indicate flow potential is upwards, positive values indicate flow potential is downwards.

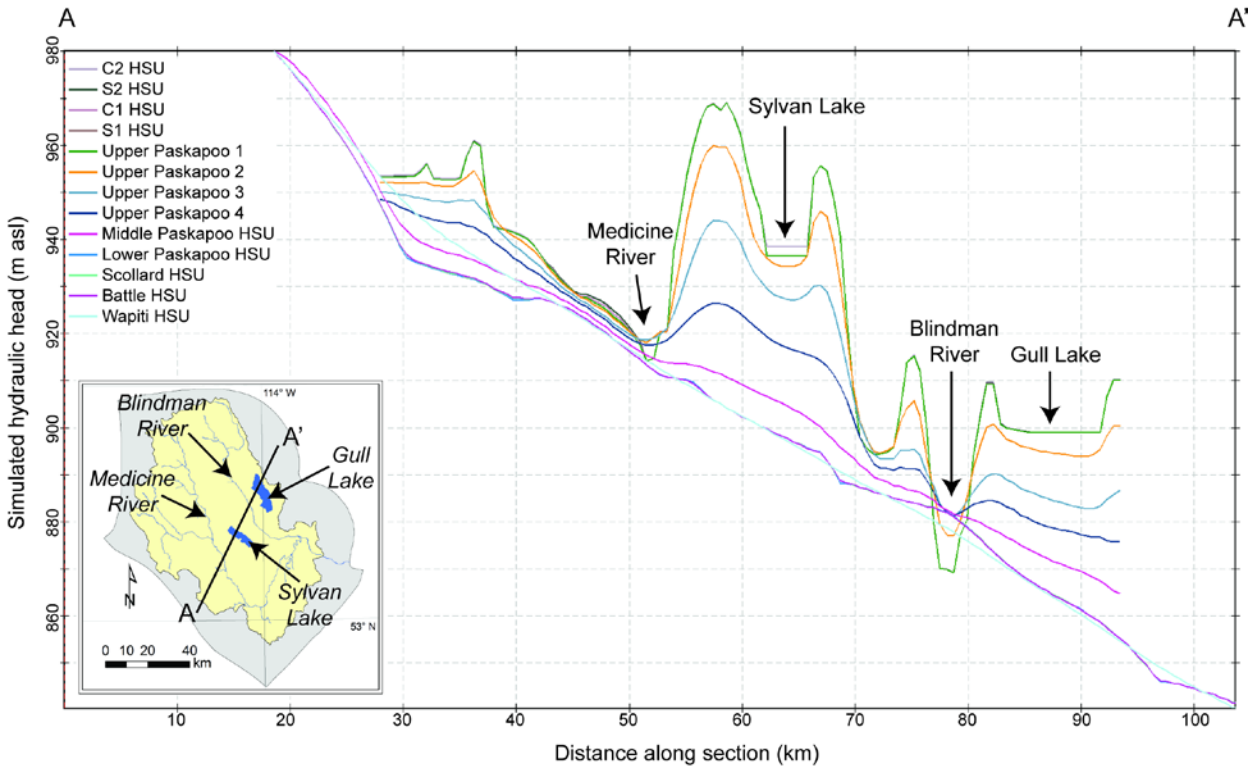

Figure 22. Simulated vertical hydraulic head distribution along cross-section A–A' in steady-state model, Sylvan Lake sub-basin, central Alberta. Abbreviation: HSU, hydrostratigraphic unit.

5.1.2 Transient Model

The results of the transient model show variation in hydraulic head in response to variations in monthly recharge and pumping (Figures 17, 18, and 23). The hydraulic heads are generally the highest in the fall months following spring and summer recharge, and lowest in the spring and early summer (Figure 17); whereas lake levels peak in the summer with direct precipitation, and reach a minimum in December (Figure 18). Figure 23 shows an example of the seasonal difference in water table elevation from November 30, 1998 to August 31, 1999. The water table is higher in November than August and the largest differences in water table elevation are found in the elevated areas.

Figure 24 shows the average monthly water budget for the five-year transient simulation. The largest fluxes are recharge into the model domain and subsequent increases and decreases in storage. There is a net flux into the model from the specified head boundaries on the southwest side of the domain, and a net loss of groundwater to rivers (negative river leakage). Groundwater lost through pumping wells represents a small portion of the overall water budget, but localized impacts of pumping may still occur (although such impacts have not been examined in detail in this report).

Average annual simulated groundwater flow into and out of Sylvan Lake is 7.9×10^5 and 1.2×10^5 m^3/yr, respectively. These values are much lower than the average values found by Baker (2009) using geochemical mass balance methods (chloride, oxygen isotopes, deuterium isotopes): 13.3×10^6 m^3/yr for groundwater inflow to the lake and 15.4×10^6 m^3/yr for outflow to groundwater. This indicates that simulation of groundwater–lake interactions could be improved upon in the numerical model, which is not surprising given the regional scope of the current version of the model.

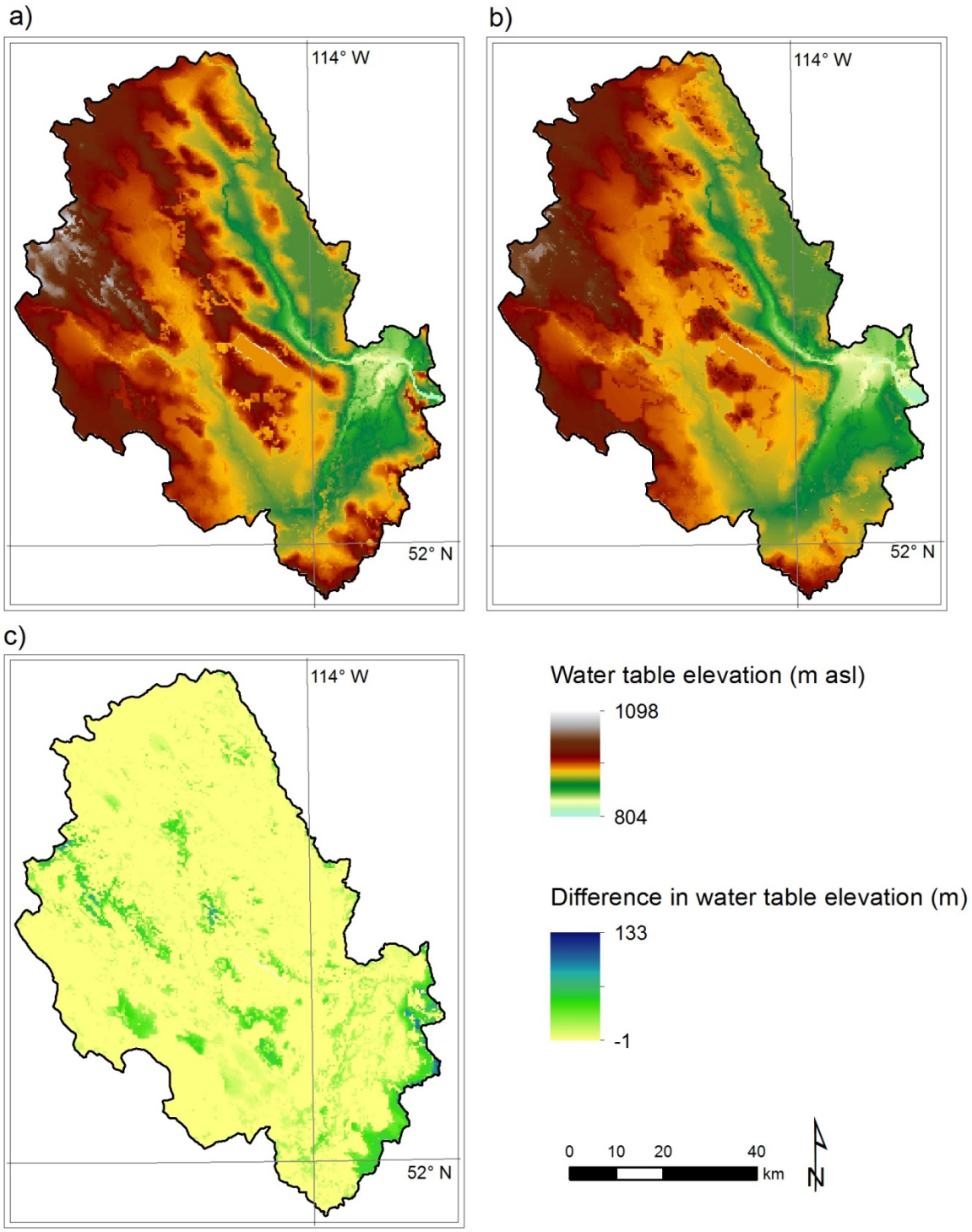

Figure 23. Example of hydraulic head difference between winter and summer (November 30, 1998 and August 31, 1999) in the Sylvan Lake sub-basin, central Alberta: a) simulated water table elevation (hydraulic head) on November 30, 1998, b) simulated water table elevation on August 31, 1999, and c) difference between the two seasonal simulated water table elevations. Positive values indicate a decrease in water table elevation from November to August.

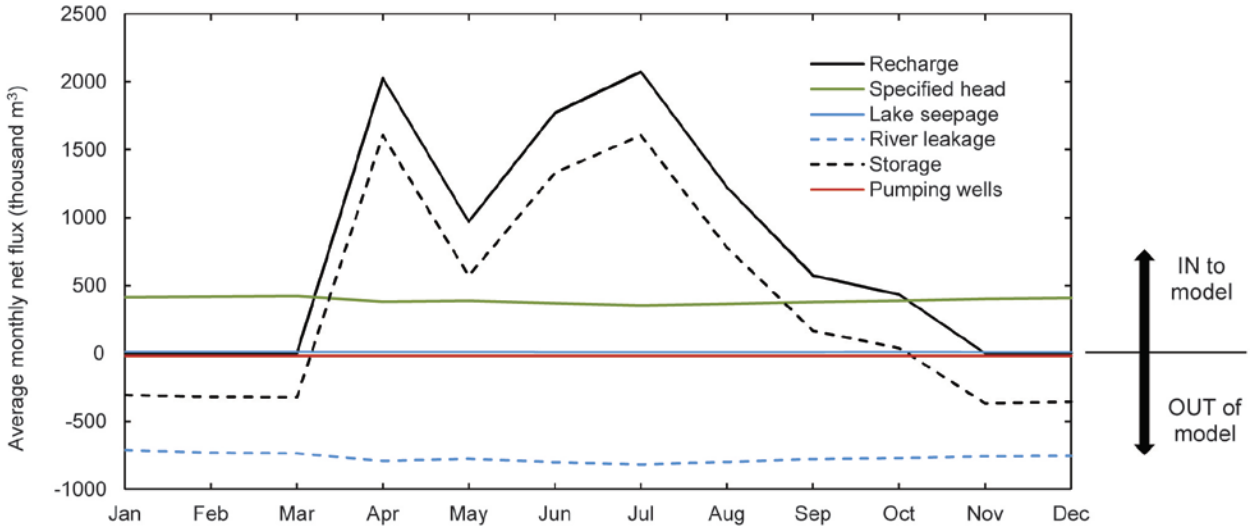

Figure 24. Average monthly net flux of various water budget components in the Sylvan Lake sub-basin, central Alberta, for the transient model simulation period from January 1, 1995 to December 31, 1999.

6 Model Limitations and Future Considerations

This model provides a tool for understanding groundwater movement in the SLSB. It was not developed to be all-encompassing of all groundwater processes at all scales, and can be adapted and built upon by stakeholders to include more complex or detailed processes and data.

Hydrostratigraphic surfaces generated for this study have inherent geostatistical uncertainty. Details on the limitations of the hydrostratigraphic model can be found in Atkinson and Glombick (2015a). Values for the specified head boundary condition along the edges of the deep domain were extracted from the regional groundwater model by Singh et al. (2014), which are consistent with provincial-scale mapping of hydraulic head conditions in the Wapiti HSU (Singh and Nakevska, in press). The understanding of regional groundwater flow beyond the lateral boundaries of the deep domain are based on relatively sparse measurements.

Uncertainty in the input parameters such as recharge, river and lake parameters, and groundwater withdrawals contributes to the uncertainty of the model; however, better calibration of the transient model may help to reduce some of this uncertainty. Land cover, which affects evapotranspiration, was not accounted for in the determination of recharge. There is also considerable uncertainty in the volume of groundwater pumping as actual pumping volumes, rates, and times are not available for unlicenced wells, and only maximum (not actual) pumping volumes are available for licenced wells. Additionally, return flow from these wells was not considered in this study.

This study uses MODFLOW RIV and LAK3 packages for simulating major surface water features in the model domain. All rivers were assigned uniform depth and riverbed conductance (i.e., uniform width, segment length, channel bed thickness and conductivity). A similar approach was taken for the two lakes in the sub-basin. This approach presents another factor that needs to be taken into account during the analysis of model results.

The lack of both spatially distributed and temporally coincident transient calibration data considerably limits the model calibration and validation. Whereas hydraulic conductivities were calibrated using automated techniques, other hydrogeological parameters such as specific storage, specific yield, and riverbed and lakebed conductances were manually calibrated within reasonable ranges. The ranges for these parameters were based on relatively scarce field data and existing literature. This lack of quantitative knowledge along with lack of calibration data limits the confidence in the model calibration.

The model simulated temporal and spatial changes in simulated water levels and is considered valid only for the set of properties and stresses used in this model.

There is also a lack of observed hydraulic heads in the deeper HSUs, such as the lower Paskapoo and Scollard. The drillstem test data from oil and gas wells available for the Wapiti HSU (e.g., Singh and Nakevska, in press) come from the hydrocarbon-dominated area of lower pressures/hydraulic heads attributed to "underpressuring" (Bachu and Underschultz, 1995; Singh and Nakevska, in press). This underpressured zone was not represented in the SLSB model because 1) the focus was on the upper HSUs; and 2) the influence of this underpressured zone operates at a geological timescale, far beyond the scope of this model.

Improvements to the model could be undertaken as additional data become available through further processing of available data, acquisition of new data sources, or gathering of field data. Possible improvements to the model include

- incorporating spatially and time varying river stages;
- incorporating spatially variable riverbed conductance;
- inclusion of the stream (STR) or streamflow-routing (SFR) package for rivers, which would account for downstream river flow;
- implementation of spatially varying recharge in the transient simulation;
- inclusion of the evapotranspiration (EVT) package to explicitly calculate groundwater evapotranspiration;
- improving the representation of lake–groundwater interactions with more detailed analysis of the influence of precipitation, evaporation, and lakebed conductance on lake–groundwater interactions;
- running the model for a different or extended time period and comparing or calibrating the simulations to available observation data;
- improving estimates of groundwater pumping and return flow;
- inclusion of additional measurements of hydraulic head or hydraulic conductivity in the deeper HSUs; and
- more rigorous uncertainty analysis.

7 Summary

The SLSB faces increasing pressure on groundwater resources due to potentially competing demands from agriculture, industry, and an increase in domestic users from population growth. The AGS has developed a numerical groundwater model of the area to serve as a tool in understanding groundwater resources in the basin. The numerical model simulates groundwater flow in 10 HSUs, including 4 N–Q sediments HSUs, based on previous work by Atkinson and Glombick (2015a). Spatial heterogeneity of the Sunchild and Haynes aquifers within the Paskapoo Formation, the uppermost bedrock unit, was accounted for. Both steady-state and transient versions of the model were developed and include net recharge, basic processes of surface water–groundwater interaction with major rivers and lakes, and groundwater pumping (transient model only). The model results show the influence of local groundwater flow systems, recharging in the topographically high areas and discharging to the rivers, and the deeper intermediate and regional flow systems. Recharge is the dominant flux into the model, followed by a net flow in through the specified head boundaries. Groundwater discharge to rivers is the dominant flow out of the model. This model is available from the AGS and aims to provide a foundation upon which local stakeholders can build upon by improving aspects of the model required for specific problems or questions.

8 References

Agriculture and Agri-Food Canada (2012): AAFC Watershed Project – 2012; Agriculture and Agri-Food Canada, watershed-related databases.

Alberta Agriculture and Forestry (2014): Current and historical Alberta weather station data; Alberta Climate Information Service, URL <http://agriculture.alberta.ca/acis/> [March 2014].

Alberta Environment and Parks (2015a): Alberta Water Well Information Database; Alberta Environment and Parks, URL <http://aep.alberta.ca/water/reports-data/alberta-water-well-information-database/default.aspx> [August 2015].

Alberta Environment and Parks (2015b): Base Features, hydrography; AltaLIS Ltd., scale 1:20 000, URL <http://www.altalis.com/products/> [August 2015].

Alberta Environment and Parks (2015c): Groundwater Observation Well Network; Alberta Environment and Parks, URL <http://aep.alberta.ca/water/programs-and-services/groundwater/groundwater-observation-well-network/default.aspx> [August 2015].

Alberta Environment and Parks (2015d): Provincial digital elevation model; AltaLIS Ltd., 25 m cell, Esri grid format, URL <http://www.altalis.com/products/terrain/dem.html> [August 2015].

Andriashek, L.D. and Lyster, S. (2012a): Structure top of the Sunchild aquifer, Alberta (gridded data, ASCII format); Alberta Energy Regulator, AER/AGS Digital Data 2015-0024, URL <https://ags.aer.ca/publications/DIG_2012_0024.html> [October 2015].

Andriashek, L.D. and Lyster, S. (2012b): Isopach of the Sunchild aquifer, Alberta (gridded data, ASCII format); Alberta Energy Regulator, AER/AGS Digital Data 2015-0019, URL <https://ags.aer.ca/publications/DIG_2012_0019.html > [October 2015].

Anderson, T.W. and Darling, D.A. (1954): A test of goodness-of-fit; Journal of the American Statistical Association, v. 49, p. 765–769.

Atkinson, L.A. (2015a): Sylvan Lake sub-basin hydrostratigraphic model - top of hydrostratigraphic unit C2 within the Neogene-Quaternary succession, central Alberta (gridded data, ASCII format); Alberta Energy Regulator, AER/AGS Digital Data 2015-0005, URL <https://ags.aer.ca/publications/DIG_2015_0005.html> [October 2015].

Atkinson, L.A. (2015b): Sylvan Lake sub-basin hydrostratigraphic model - top of hydrostratigraphic unit S2 within the Neogene-Quaternary succession, central Alberta (gridded data, ASCII format); Alberta Energy Regulator, AER/AGS Digital Data 2015-0016, URL <https://ags.aer.ca/publications/DIG_2015_0016.html > [October 2015].

Atkinson, L.A. (2015c): Sylvan Lake sub-basin hydrostratigraphic model - top of hydrostratigraphic unit C1 within the Neogene-Quaternary succession, central Alberta (gridded data, ASCII format); Alberta Energy Regulator, AER/AGS Digital Data 2015-0017, URL <https://ags.aer.ca/publications/DIG_2015_0017.html> [October 2015].

Atkinson, L.A. (2015d): Sylvan Lake sub-basin hydrostratigraphic model - top of hydrostratigraphic unit S1 within the Neogene-Quaternary succession, central Alberta (gridded data, ASCII format); Alberta Energy Regulator, AER/AGS Digital Data 2015-0018, URL <https://ags.aer.ca/publications/DIG_2015_0018.html> [October 2015].

Atkinson, L.A. (2015e): Sylvan Lake sub-basin hydrostratigraphic model - top of the Paskapoo Formation - upper composite slice, central Alberta (gridded data, ASCII format); Alberta Energy Regulator, AER/AGS Digital Data 2015-0019, URL <https://ags.aer.ca/publications/DIG_2015_0019.html> [October 2015].

Atkinson, L.A. and Glombick, P.M. (2015a): Three-dimensional hydrostratigraphic modelling of the Sylvan Lake sub-basin in the Edmonton-Calgary Corridor, central Alberta; Alberta Energy Regulator, AER/AGS Open File Report 2014-10, 58 p., URL <http://ags.aer.ca/publications/OFR_2014_10.html> [September 2018].

Atkinson, L.A. and Glombick, P.M. (2015b): Sylvan Lake sub-basin hydrostratigraphic model - top of the Paskapoo Formation - middle composite slice, central Alberta (gridded data, ASCII format); Alberta Energy Regulator, AER/AGS Digital Data 2015-0020, URL <https://ags.aer.ca/publications/DIG_2015_0020.html> [October 2015].

Atkinson, L.A. and Glombick, P.M. (2015c): Sylvan Lake sub-basin hydrostratigraphic nodel - top of the Paskapoo Formation - lower composite slice, central Alberta (gridded data, ASCII format); Alberta Energy Regulator, AER/AGS Digital Data 2015-0021, URL <https://ags.aer.ca/publications/DIG_2015_0021.html> [October 2015].

Atkinson, L.A. and Glombick, P.M. (2015d): Sylvan Lake sub-basin hydrostratigraphic model - distribution of greater than or equal to 0.60 net-to-gross sandstone values within the Paskapoo Formation - upper composite slice, central Alberta (gridded data, ASCII format); Alberta Energy Regulator, AER/AGS Digital Data 2015-0009, URL <https://ags.aer.ca/publications/DIG_2015_0009.html> [October 2015].

Atkinson, L.A. and Glombick, P.M. (2015e): Sylvan Lake sub-basin hydrostratigraphic model - distribution of greater than or equal to 0.60 net-to-gross sandstone values within the Paskapoo Formation - middle composite slice, central Alberta (gridded data, ASCII format); Alberta Energy Regulator, AER/AGS Digital Data 2015-0008, URL <https://ags.aer.ca/publications/DIG_2015_0008.html> [October 2015].

Atkinson, L.A. and Glombick, P.M. (2015f): Sylvan Lake sub-basin hydrostratigraphic model - distribution of greater than or equal to 0.60 net-to-gross sandstone values within the Paskapoo Formation - lower composite slice, central Alberta (gridded data, ASCII format); Alberta Energy Regulator, AER/AGS Digital Data 2015-0007, URL <https://ags.aer.ca/publications/DIG_2015_0007.html> [October 2015].

Atkinson, L.A. and MacCormack, K.E. (2015a): Sylvan Lake sub-basin hydrostratigraphic model - top of the Scollard Formation, central Alberta (gridded data, ASCII format); Alberta Energy Regulator, AER/AGS Digital Data 2015-0006, URL <https://ags.aer.ca/publications/DIG_2015_0006.html> [October 2015].

Atkinson, L.A. and MacCormack, K.E. (2015b): Sylvan Lake sub-basin hydrostratigraphic model - top of the Battle Formation, central Alberta (gridded data, ASCII format); Alberta Energy Regulator, AER/AGS Digital Data 2015-0013, URL <https://ags.aer.ca/publications/DIG_2015_0013.html> [October 2015].

Atkinson, L.A. and MacCormack, K.E. (2015c): Sylvan Lake sub-basin hydrostratigraphic model - top of the Wapiti Formation, central Alberta (gridded data, ASCII format); Alberta Energy Regulator, AER/AGS Digital Data 2015-0014, URL <https://ags.aer.ca/publications/DIG_2015_0014.html> [October 2015].

Atkinson, L.A. and MacCormack, K.E. (2015d): Sylvan Lake sub-basin hydrostratigraphic model - top of the Lea Park Formation, central Alberta (gridded data, ASCII format); Alberta Energy Regulator, AER/AGS Digital Data 2015-0015, URL <https://ags.aer.ca/publications/DIG_2015_0015.html> [October 2015].

AXYS Environmental Consulting Ltd. (2005): Sylvan Lake water quality assessment and watershed management considerations; unpublished report prepared for Lacombe County, 441 p., URL <https://www.lacombecounty.com/index.php/studies/134-sylvan-lake-water-quality-assessment-and-watershed-management-considerations> [September 2017].

Bachu, S. and Underschultz, J.R. (1995): Large-scale underpressuring in the Mississippian–Cretaceous succession, southwestern Alberta Basin; American Association of Petroleum Geologists, Bulletin, v. 79, p. 989–1004.

Baker, J.L. (2009): Groundwater contribution to Sylvan Lake, Alberta, Canada; M.Sc. thesis, University of Calgary, 104 p.

Barker, A.A., Riddell, J.T.F., Slattery, S.R., Andriashek, L.D., Moktan, H., Wallace, S., Lyster, S., Jean, G., Huff, G.F., Stewart, S.A. and Lemay, T.G. (2011): Edmonton-Calgary Corridor groundwater atlas; Energy Resources Conservation Board, ERCB/AGS Information Series 140, 98 p., URL <http://ags.aer.ca/publications/INF_140.html> [September 2018].

Chen, Z., Grasby, T., Hamblin, T. and Xiu, S. (2007): Paskapoo groundwater study, part II: sandstone thickness and porosity estimations using well log data for the aquifer system in the Tertiary Paskapoo Formation, Alberta; Geological Survey of Canada, Open File Report 5445, 14 p., doi:10.4095/223560.

Dawson, F.M., Evans, C.G., Marsh, R. and Richardson, R. (1994): Uppermost Cretaceous and Tertiary strata of the Western Canada Sedimentary Basin; *in* Geological atlas of the Western Canada Sedimentary Basin, G.D. Mossop and I. Shetsen (comp.), Canadian Society of Petroleum Geologists and Alberta Research Council, p. 387–406, URL <http://ags.aer.ca/publications/chapter-24-uppermost-cretaceous-and-tertiary-strata.htm> [September 2018].

Deltares (2015): iMOD; Deltares, modelling software, URL <https://www.deltares.nl/en/software/imod/> [September 2018].

Demchuk, T.D. and Hills, L. (1991): A re-examination of the Paskapoo Formation in the central Alberta Plains: the designation of three new members; Bulletin of Canadian Petroleum Geology, v. 39, no. 3, p. 270–282, URL <http://archives.datapages.com/data/cspg/data/039/039003/0270.htm> [September 2018].

Environment Canada (2015): 1981–2010 Canadian climate normals and averages; Environment Canada, URL <http://climate.weather.gc.ca/climate_normals/index_e.html> [August 2015].

Esri (2012): ArcGIS 10.1; Esri, mapping platform, URL <http://www.esri.ca/> [September 2018].

Grasby, S.E., Chen, Z., Hamblin, A.P., Wozniak, P.R.J. and Sweet, A.R. (2008): Regional characterization of the Paskapoo bedrock aquifer system, southern Alberta; Canadian Journal of Earth Sciences, v. 45, no. 12, p. 1501–1516, doi:10.1139/E08-069.

Harbaugh, A.W. (1990): A computer program for calculating subregional water budgets using results from the U.S. Geological Survey modular three-dimensional finite- difference ground-water flow model; United States Geological Survey, Open-File Report 90-392, 46 p., doi:10.3133/ofr90392.

Harbaugh, A.W., Banta, E.R., Hill, M.C. and McDonald, M.G. (2000): MODFLOW-2000, the U.S. Geological Survey modular ground-water model - user guide to modularization concepts and the ground-water flow process; United States Geological Survey, Open-File Report 2000-92, 121 p., doi:10.3133/ofr200092.

Hathway, B. (2011): Tops of the Horseshoe Canyon, Wapiti and Battle formations in the west-central Alberta Plains: subsurface stratigraphic picks and modelled surface; Energy Resources Conservation Board, ERCB/AGS Open File Report 2011-08, 24 p., URL <http://ags.aer.ca/publications/OFR_2011_08.html> [September 2018].

Hydrogeological Consultants Ltd. (2001): Lacombe County, Part of the Red Deer River Basin, Tp 038 to 041, R 21 to 28, W4M & Tp 038 to 041, R 01 to 04, W5M, regional groundwater assessment; unpublished report prepared for Lacombe County, 46 p., URL <https://www.hcl.ca/public/download/documents/11740> [September 2018].

Hydrogeological Consultants Ltd. (2005): Red Deer County, Part of the Red Deer River Basin, Tp 034 to 039, R 21 to 28, W4M and Tp 034 to 039, R 01 to 04, W5M, regional groundwater assessment; unpublished report prepared for Red Deer County, 64 p., URL <https://www.hcl.ca/public/download/documents/11766> [September 2018].

Lyster, S. and Andriashek, L.D. (2012): Geostatistical rendering of the architecture of hydrostratigraphic units within the Paskapoo Formation, central Alberta; Energy Resources Conservation Board, ERCB/AGS Bulletin 66, 115 p., URL <http://ags.aer.ca/publications/BUL_066.html> [September 2018].

Merritt, M.L. and Konikow, L.F. (2000): Documentation of a computer program to simulate lake–aquifer interaction using the MODFLOW ground water flow model and the MOC3D solute-transport model; United States Geological Survey, Water-Resources Investigations Report 00-4167, 146 p., doi:10.3133/wri004167.

Michael, K. and Bachu, S. (2001): Fluids and pressure distributions in the foreland-basin succession in the west-central part of the Alberta basin, Canada: evidence for permeability barriers and hydrocarbon generation and migration; American Association of Petroleum Geologists, Bulletin, v. 85, no. 7, p. 1231–1252, URL <http://archives.datapages.com/data/bulletns/2001/07jul/1231/1231.htm> [September 2018].

Natural Regions Committee (2006): Natural regions and subregions of Alberta; Government of Alberta, D.J. Downing and W.W. Pettapiece (comp.), Publication Number T/852, 254 p., URL <https://open.alberta.ca/publications/0778545725> [September 2017].

Niswonger, R.G., Panday, S. and Ibaraki, M. (2011): MODFLOW-NWT, a Newton formulation for MODFLOW-2005; United States Geological Survey, Techniques and Methods 6-A37, 44 p., URL <https://pubs.usgs.gov/tm/tm6a37/> [September 2018].

Pettapiece, W.W. (1986): Physiographic subdivisions of Alberta; Agriculture Canada, Research Branch, Land Resource Research Centre.

Riddell, J.T.F. and Lyster, S. (2017): Hydrogeological overview of the Edmonton–Calgary Corridor, central Alberta; Alberta Energy Regulator, AER/AGS Open File Report 2017-05, 25 p., URL <http://ags.aer.ca/OFR_2017_05.html> [September 2018].

Riddell, J.T.F., Andriashek, L.D., Jean, G. and Slattery, S.R. (2009): Preliminary results of sediment coring in the Edmonton–Calgary Corridor, central Alberta; Energy Resources Conservation Board, ERCB/AGS Open File Report 2009-17, 81 p., URL <http://ags.aer.ca/publications/OFR_2009_17.html> [September 2018].

Riddell, J.T.F., Moktan, H. and Jean, G. (2014): Regional hydrology of the Edmonton–Calgary Corridor, Alberta; Alberta Energy Regulator, AER/AGS Open File Report 2014-02, 31 p., URL <http://ags.aer.ca/publications/OFR_2014_02.html> [September 2018].

Singh, A. and Nakevska, N. (in press): Distribution of hydraulic head in the Wapiti / Belly River hydrostratigraphic unit; Alberta Energy Regulator / Alberta Geological Survey, AER/AGS Map 543, scale 1:1 750 000.

Singh, A., Palombi, D. and Huff, G.F. (2014): Application of response surface based calibration methods for regional hydrogeological modelling in the Western Canada Sedimentary Basin; poster presented at American Geophysical Union fall meeting, December 15–19, 2014, San Francisco, California, URL <http://ags.aer.ca/document/Presentations/PR_Singh_SARGS.pdf> [September 2018].

Smerdon, B.D., Hughes, A.T. and Jean, G. (2017): Permeability measurements of Upper Cretaceous and Paleogene bedrock cores made from 2004-2015 (tabular data, tab-delimited format, to accompany Open File Report 2016-03); Alberta Energy Regulator, AER/AGS Digital Data 2016-0042, URL <http://ags.aer.ca/DIG-2016-0042.html> [September 2018].

Tolson, B.A. and Shoemaker, C.A. (2007): Dynamically dimensioned search algorithm for computationally efficient watershed model calibration; Water Resources Research, v. 43, issue 1, doi:10.1029/2005WR004723.

van der Kamp, G. and Hayashi, M. (1998): The groundwater recharge function of small wetlands in the semi-arid northern prairies; Great Plains Research: A Journal of Natural and Social Sciences, v. 8, no. 1, p. 39–56, URL <http://digitalcommons.unl.edu/greatplainsresearch/366/?utm_source=digitalcommons.unl.edu%2Fgreatplainsresearch%2F366&utm_medium=PDF&utm_campaign=PDFCoverPages> [September 2018].

Waterloo Hydrogeologic (2016): Visual MODFLOW Classic, Build 4.6.0.168; Waterloo Hydrogeologic, modelling software, URL <https://www.waterloohydrogeologic.com/> [September 2018].

Water Survey of Canada (2017): HYDAT database; Water Survey of Canada, URL <https://www.ec.gc.ca/rhc-wsc/> [July 2017].